References

Akiyama, H., Chaboissier, M. C., Martin, J. F., Schedl, A. and de Crombrugghe, B. (2002). The transcription factor Sox9 has essential roles in successive steps of the chondrocyte differentiation pathway and is required for expression of Sox5 and Sox6. *Genes Dev.* **16**, 2813-2828.

Akiyama, H., Lyons, J. P., Mori-Akiyama, Y., Yang, X., Zhang, R., Zhang, Z., Deng, J. M., Taketo, M. M., Nakamura, T., Behringer, R. R. et al. (2004). Interactions between Sox9 and beta-catenin control chondrocyte differentiation. *Genes Dev.* **18**, 1072-1087.

Akiyama, H., Kim, J. E., Nakashima, K., Balmes, G., Iwai, N., Deng, J. M., Zhang, Z., Martin, J. F., Behringer, R. R., Nakamura, T. et al. (2005). Osteo-chondroprogenitor cells are derived from Sox9 expressing precursors. *Proc. Natl. Acad. Sci. USA* **102**, 14665-14670.

Bi, W., Deng, J. M., Zhang, Z., Behringer, R. R. and de Crombrugghe, B. (1999). Sox9 is required for cartilage formation. *Nat. Genet.* **22**, 85-89.

Bi, W., Huang, W., Whitworth, D. J., Deng, J. M., Zhang, Z., Behringer, R. R. and de Crombrugghe, B. (2001). Haploinsufficiency of Sox9 results in defective cartilage primordia and premature skeletal mineralization. *Proc. Natl. Acad. Sci. USA* **98**, 6698-6703.

Brazil, D. P., Yang, Z. Z. and Hemmings, B. A. (2004). Advances in protein kinase B signalling: AKTion on multiple fronts. *Trends Biochem. Sci.* **29**, 233-242.

Brew, C. J., Clegg, P. D., Boot-Handford, R. P., Andrew, J. G. and Hardingham, T. (2010). Gene expression in human chondrocytes in late osteoarthritis is changed in both fibrillated and intact cartilage without evidence of generalised chondrocyte hypertrophy. *Ann. Rheum. Dis.* **69**, 234-240.

Cantley, L. C. (2002). The phosphoinositide 3-kinase pathway. *Science* **296**, 1655-1657.

Chen, W. S., Xu, P. Z., Gottlob, K., Chen, M. L., Sokol, K., Shiyanova, T., Roninson, I., Weng, W., Suzuki, R., Tobe, K. et al. (2001). Growth retardation and increased apoptosis in mice with homozygous disruption of the Akt1 gene. *Genes Dev.* **15**, 2203-2208.

Cheung, M., Chaboissier, M. C., Mynett, A., Hirst, E., Schedl, A. and Briscoe, J. (2005). The transcriptional control of trunk neural crest induction, survival, and delamination. *Dev. Cell* **8**, 179-192.

Ducy, P., Zhang, R., Geoffroy, V., Ridall, A. L. and Karsenty, G. (1997). Osf2/Cbfa1: a transcriptional activator of osteoblast differentiation. *Cell* **89**, 747-754.

Ford-Hutchinson, A. F., Ali, Z., Lines, S. E., Hallgrimsson, B., Boyd, S. K. and Jirik, F. R. (2007). Inactivation of Pten in osteo-chondroprogenitor cells leads to epiphyseal growth plate abnormalities and skeletal overgrowth. *J. Bone Miner. Res.* **22**, 1245-1259.

Foster, J. W., Dominguez-Steglich, M. A., Guioli, S., Kwok, C., Weller, P. A., Stevanovic, M., Weissenbach, J., Mansour, S., Young, I. D., Goodfellow, P. N. et al. (1994). Campomelic dysplasia and autosomal sex reversal caused by mutations in an SRY-related gene. *Nature* **372**, 525-530.

Fujita, T., Azuma, Y., Fukuyama, R., Hattori, Y., Yoshida, C., Koida, M., Ogita, K. and Komori, T. (2004). Runx2 induces osteoblast and chondrocyte differentiation and enhances their migration by coupling with PI3K-Akt signaling. *J. Cell Biol.* **166**, 85-95.

Fukai, A., Kawamura, N., Saito, T., Oshima, Y., Ikeda, T., Kugimiya, F., Higashikawa, A., Yano, F., Ogata, N., Nakamura, K. et al. (2010). Akt1 in murine chondrocytes controls cartilage calcification during endochondral ossification under physiologic and pathologic conditions. *Arthritis Rheum.* **62**, 826-836.

Hattori, T., Muller, C., Gebhard, S., Bauer, E., Pausch, F., Schlund, B., Bosl, M. R., Hess, A., Surmann-Schmitt, C., von der Mark, H. et al. (2010). SOX9 is a major negative regulator of cartilage vascularization, bone marrow formation and endochondral ossification. *Development* **137**, 901-911.

Hui, R. C., Gomes, A. R., Constantinidou, D., Costa, J. R., Karadedou, C. T., Fernandez de Mattos, S., Wymann, M. P., Brosens, J. J., Schulze, A. and Lam, E. W. (2008). The forkhead transcription factor FOXO3a increases phosphoinositide-3 kinase/Akt activity in drug-resistant leukemic cells through induction of PIK3CA expression. *Mol. Cell. Biol.* **28**, 5886-5898.

Iwai, T., Murai, J., Yoshikawa, H. and Tsumaki, N. (2008). Smad7 Inhibits chondrocyte differentiation at multiple steps during endochondral bone formation and down-regulates p38 MAPK pathways. *J. Biol. Chem.* **283**, 27154-27164.

Kita, K., Kimura, T., Nakamura, N., Yoshikawa, H. and Nakano, T. (2008). PI3K/Akt signaling as a key regulatory pathway for chondrocyte terminal differentiation. *Genes Cells* **13**, 839-850.

Lefebvre, V. and Smits, P. (2005). Transcriptional control of chondrocyte fate and differentiation. *Birth Defects Res. C Embryo Today* **75**, 200-212.

Miller, S. J., Jessen, W. J., Mehta, T., Hardiman, A., Sites, E., Kaiser, S., Jegga, A. G., Li, H., Upadhyaya, M., Giovannini, M. et al. (2009). Integrative genomic analyses of neurofibromatosis tumours identify SOX9 as a biomarker and survival gene. *EMBO Mol. Med.* **1**, 236-248.

Ng, L. J., Wheatley, S., Muscat, G. E., Conway-Campbell, J., Bowles, J., Wright, E., Bell, D. M., Tam, P. P., Cheah, K. S. and Koopman, P. (1997). SOX9 binds DNA, activates transcription, and coexpresses with type II collagen during chondrogenesis in the mouse. *Dev. Biol.* **183**, 108-121.

Pelton, R. W., Dickinson, M. E., Moses, H. L. and Hogan, B. L. (1990). In situ hybridization analysis of TGF beta 3 RNA expression during mouse development: comparative studies with TGF beta 1 and beta 2. *Development* **110**, 609-620.

Peng, X. D., Xu, P. Z., Chen, M. L., Hahn-Windgassen, A., Skeen, J., Jacobs, J., Sundararajan, D., Chen, W. S., Crawford, S. E., Coleman, K. G. et al. (2003). Dwarfism, impaired skin development, skeletal muscle atrophy, delayed bone development, and impeded adipogenesis in mice lacking Akt1 and Akt2. *Genes Dev.* **17**, 1352-1365.

Peters, P. W. J. (1977). Double staining of fetal skeletons for cartilage and bone. In *Methods in Prenatal Toxicology* (ed. H. J. M. D. Neuberg and T. E. Kwasigroch), pp. 153-154. Stuttgart, Germany: Georg Thieme Verlag.

Rokutanda, S., Fujita, T., Kanatani, N., Yoshida, C. A., Komori, H., Liu, W., Mizuno, A. and Komori, T. (2009). Akt regulates skeletal development through GSK3, mTOR, and FoxOs. *Dev. Biol.* **328**, 78-93.

Sakai, K. and Miyazaki, J. (1997). A transgenic mouse line that retains Cre recombinase activity in mature oocytes irrespective of the cre transgene transmission. *Biochem. Biophys. Res. Commun.* **237**, 318-324.

Shukunami, C., Shigeno, C., Atsumi, T., Ishizeki, K., Suzuki, F. and Hiraki, Y. (1996). Chondrogenic differentiation of clonal mouse embryonic cell line ATDC5 in vitro: differentiation-dependent gene expression of parathyroid hormone (PTH)/PTH-related peptide receptor. *J. Cell Biol.* **133**, 457-468.

Smits, P., Li, P., Mandel, J., Zhang, Z., Deng, J. M., Behringer, R. R., de Crombrugghe, B. and Lefebvre, V. (2001). The transcription factors L-Sox5 and Sox6 are essential for cartilage formation. *Dev. Cell* **1**, 277-290.

Smits, P., Dy, P., Mitra, S. and Lefebvre, V. (2004). Sox5 and Sox6 are needed to develop and maintain source, columnar, and hypertrophic chondrocytes in the cartilage growth plate. *J. Cell Biol.* **164**, 747-758.

Suzuki, A., Yamaguchi, M. T., Ohteki, T., Sasaki, T., Kaisho, T., Kimura, Y., Yoshida, R., Wakeham, A., Higuchi, T., Fukumoto, M. et al. (2001). T cell-specific loss of Pten leads to defects in central and peripheral tolerance. *Immunity* **14**, 523-534.

Thomsen, M. K., Ambroisine, L., Wynn, S., Cheah, K. S., Foster, C. S., Fisher, G., Berney, D. M., Moller, H., Reuter, V. E., Scardino, P. et al. (2010). SOX9 elevation in the prostate promotes proliferation and cooperates with PTEN loss to drive tumor formation. *Cancer Res.* **70**, 979-987.

Ulici, V., Hoenselaar, K. D., Gillespie, J. R. and Beier, F. (2008). The PI3K pathway regulates endochondral bone growth through control of hypertrophic chondrocyte differentiation. *BMC Dev. Biol.* **8**, 40.

Wagner, T., Wirth, J., Meyer, J., Zabel, B., Held, M., Zimmer, J., Pasantes, J., Bricarelli, F. D., Keutel, J., Hustert, E. et al. (1994). Autosomal sex reversal and campomelic dysplasia are caused by mutations in and around the SRY-related gene SOX9. *Cell* **79**, 1111-1120.

Wang, Y. and Sul, H. S. (2009). Pref-1 regulates mesenchymal cell commitment and differentiation through Sox9. *Cell Metab.* **9**, 287-302.

Yang, G., Sun, Q., Teng, Y., Li, F., Weng, T. and Yang, X. (2008). PTEN deficiency causes dyschondroplasia in mice by enhanced hypoxia-inducible factor 1alpha signaling and endoplasmic reticulum stress. *Development* **135**, 3587-3597.

Zhao, Q., Eberspaecher, H., Lefebvre, V. and De Crombrugghe, B. (1997). Parallel expression of Sox9 and Col2a1 in cells undergoing chondrogenesis. *Dev. Dyn.* **209**, 377-386.

Zheng, Q., Zhou, G., Morello, R., Chen, Y., Garcia-Rojas, X. and Lee, B. (2003). Type X collagen gene regulation by Runx2 contributes directly to its hypertrophic chondrocyte-specific expression in vivo. *J. Cell Biol.* **162**, 833-842.

Zhou, G., Zheng, Q., Engin, F., Munivez, E., Chen, Y., Sebald, E., Krakow, D. and Lee, B. (2006). Dominance of SOX9 function over RUNX2 during skeletogenesis. *Proc. Natl. Acad. Sci. USA* **103**, 19004-19009.

Bone 48 (2011) 476–484

Contents lists available at ScienceDirect

Bone

journal homepage: www.elsevier.com/locate/bone

PKCα suppresses osteoblastic differentiation

Akio Nakura, Chikahisa Higuchi *, Kiyoshi Yoshida, Hideki Yoshikawa

Department of Orthopaedic Surgery, Graduate School of Medicine, Osaka University, Suita, Osaka, Japan

ARTICLE INFO

Article history:
Received 11 May 2010
Revised 8 September 2010
Accepted 29 September 2010
Available online 14 October 2010

Edited by: Toshio Matsumoto

Keywords:
PKCα
MC3T3-E1 cells
Osteoblastic differentiation
Osteoblastic cell proliferation
Signal transduction

ABSTRACT

Protein kinase C (PKC) plays an essential role in cellular signal transduction for mediating a variety of biological functions. There are 11 PKC isoforms and these isoforms are believed to play distinct roles in cells. Although the role of individual isoforms of PKC has been investigated in many fields, little is known about the role of PKC in osteoblastic differentiation. Here, we investigated which isoforms of PKC are involved in osteoblastic differentiation of the mouse preosteoblastic cell line MC3T3-E1. Treatment with Gö6976, an inhibitor of PKCα and PKCβI, increased alkaline phosphatase (ALP) activity as well as gene expression of ALP and Osteocalcin (OCN), and enhanced calcification of the extracellular matrix. Concurrently, osteoblastic cell proliferation decreased at a concentration of 1.0 μM. In contrast, a PKCβ inhibitor, which inhibits PKCβI and PKCβII, did not significantly affect osteoblastic differentiation or cell proliferation. Knockdown of PKCα using MC3T3-E1 cells transfected with siRNA also induced an increase in ALP activity and in gene expression of ALP and OCN. In contrast, overexpression of wild-type PKCα decreased ALP activity and attenuated osteoblastic differentiation markers including ALP and OCN, but promoted cell proliferation. Taken together, our results indicate that PKCα suppresses osteoblastic differentiation, but promotes osteoblastic cell proliferation. These results imply that PKCα may have a pivotal role in cell signaling that modulates the differentiation and proliferation of osteoblasts.

© 2010 Elsevier Inc. All rights reserved.

Introduction

Protein kinase C (PKC) is a serine/threonine protein kinase that is known to be involved in multiple cellular signal transduction pathways that mediate cellular functions such as proliferation and differentiation [1–4]. PKC was first purified from bovine cerebellum in 1977 as a new species of protein kinase [5], following which, it was shown to be expressed in many other tissues [6]. To date, 11 PKC isoforms have been identified, which are classified into three groups based on their structure and cofactor regulation [7,8]: conventional PKC (α, βI, βII, and γ), novel PKC (δ, ε, η, θ, and μ), and atypical PKC (ζ and λ). Conventional PKCs are Ca^{2+}-dependent and are activated by both phosphatidylserine (PS) and the second messenger diacylglycerol (DAG). Novel PKCs are regulated by PS and DAG, but their activation is Ca^{2+}-independent. Atypical PKCs require neither Ca^{2+} nor PS and DAG for activation. Although some PKC isoforms are cell-type specific, PKCα, δ, ε, and ζ seem to be ubiquitous [7,9].

The role of each PKC isoform has been mostly evaluated in a variey of fields using genetic and molecular approaches employing isoform-specific inhibitors [10–12], isoform-specific RNAi and/or isoform overexpression. Much progress has been made in clinical studies of the role of PKC isoforms in cardiovascular disease and tumorigenesis and some isoforms of PKC are currently being used as theraupic targets [13]. For example, a selective inhibitor of PKCβ is under evaluation in a clinical trial as a theraupic agent for diabetic complications [14,15]. Although such systemic diseases often involve a change in bone quantity and quality, little is known about the effects of PKC on bone formation. Expression of PKC isoforms in osteoblasts has been reported [4,16], suggesting that a therapeutic agent targeted towards specific PKC isoforms might inadvertently modulate bone formation. Conversely, if the involvement of isoforms of PKC in bone formation are understood, a new agent for the regulation of bone formation might be developed.

Our purpose was to determine which isoforms of PKC play an important role in osteoblastic differentiation. In the present paper, we mainly investigated the role of PKCα and PKCβ in osteoblasts using commercially available inhibitors of PKC isoforms. We speculated that of the eleven different isoforms of PKC, PKCα in particular may have a suppressive role in osteoblastic differentiation. In addition, we confirmed this role of PKCα by knockdown of PKCα, and by overexpression of PKCα, in MC3T3-E1 cells. Meanwhile, PKCα promoted osteoblastic proliferation. Our present study indicates that PKCα suppresses osteoblastic differentiation.

* Corresponding author. Department of Orthopaedic Surgery, Graduate School of Medicine, Osaka University, 2-2 Yamadaoka, Suita, Osaka 565-0871, Japan. Fax: +81 6 6879 3559.
E-mail addresses: nakura-osaka@umin.ac.jp (A. Nakura), c-higuchi@umin.ac.jp (C. Higuchi), y_kiyoshi@csc.jp (K. Yoshida), yhideki@ort.med.osaka-u.ac.jp (H. Yoshikawa).

8756-3282/$ – see front matter © 2010 Elsevier Inc. All rights reserved.
doi:10.1016/j.bone.2010.09.238

Materials and methods

Cell culture

Mouse preosteoblastic MC3T3-E1 cells were obtained from Riken Cell Bank (Tsukuba, Japan). The cells were seeded at a concentration of 2.0×10^4 cells/cm^2 in α-minimal essential medium (α-MEM; Invitrogen, Carlsbad, CA, USA) supplemented with 10% fetal bovine serum (FBS; Hyclone, Road Logan, UT, USA) (growth medium) at 37 °C under a humidified atmosphere of 5% CO_2. For each assay, the growth medium was replaced with growth medium supplemented with 0.2 mM ascorbic acid (AA; Sigma-Aldrich, St. Louis, MO, USA) and 10 mM β-glycerophosphate (βGP; Sigma-Aldrich) (differentiation medium). The medium was changed twice per week.

Alkaline phosphatase (ALP) staining

MC3T3-E1 cells were seeded in a 24-well plate at a density of 2.0×10^4 cells/cm^2. After 24 h incubation, the cells were treated with the PKCα/PKCβI inhibitor Gö6976 (Calbiochem, San Diego, CA, USA), the PKCβ inhibitor (Calbiochem), or with 12-*O*-tetradecanoylphorbol-13-acetate (TPA; Calbiochem) in differentiation medium for 3 days. For ALP staining, cells were washed with phosphate-buffered saline (PBS; Sigma-Aldrich) and fixed for 15 min with 10% formalin at room temperature. After fixation, the cells were incubated with the ProtoBlot® II AP System with Stabilized Substrate (Promega, Madison, WI, USA) for 1 h at room temperature. For all experiments using inhibitors and activators of PKC, we also assayed the vehicle (DMSO) as a standard control [17].

ALP activity

To measure ALP activity, cells were washed twice with PBS and then lysed in mammalian protein extraction reagent (M-PER; Pierce, Rockford, IL, USA) following the manufacturer's protocol. ALP activity was measured using LabAssay™ ALP (Wako Pure Chemicals Industries, Ltd., Osaka, Japan) and p-nitrophenylphosphate as a substrate. In order to normalize enzyme activity, the protein content was measured using a bichinconinic acid (BCA) protein assay kit (Pierce).

Proliferation assay

MC3T3-E1 cells were cultured in 48-well plates at a concentration of 2.0×10^4 cells/cm^2 in differentiation medium. Cell proliferation was assessed using the Premix WST-1 cell proliferation assay system (Takara Bio, Inc., Otsu, Japan) according to the manufacturer's instructions. We performed this assay every 24 h.

Alizarin red staining

MC3T3-E1 cells were cultured for 28 days on BIOCOAT® 24-well plates (Nippon Becton Dickinson Co., Ltd., Tokyo, Japan) in differentiation medium. Then, the cells were washed twice with PBS, fixed in 10% formalin for 10 min and then stained with Alizarin Red S (Sigma-Aldrich) at pH 6.3 for 1 h. After discarding the Alizarin Red S solution and washing the cells three times with distilled water, bound Alizarin Red was dissolved in 200 μL of 100 mM hexadecylpyridium chloride (Sigma-Aldrich) and the absorbance of the supernatant was measured at 570 nm.

Reverse transcription PCR (RT-PCR) and quantitative real-time PCR

Total RNA was isolated from cells using TRIzol (Invitrogen) according to the manufacturer's instructions. cDNA was synthesized using the Transcriptor First Strand cDNA Synthesis kit (Roche Diagnostics GmbH, Mannheim, Germany). RT-PCR was performed using a PCR Master Mix (Promega) and an appropriate pair of primers. The sequences of the specific primers used for RT-PCR are shown in Table 1. PCR products were separated by agarose gel electrophoresis and stained with ethidium bromide. Each mRNA was measured using a quantitative real-time PCR assay, which employed LightCycler® TaqMan® Master (Roche Diagnostics), a Universal ProbeLibrary Probe (UPL Probe; Roche Diagnostics), an appropriate pair of primers according to the manufacturer's protocol. The sequences of specific primers and UPL Probes used are shown in Table 2. Expression values were normalized to GAPDH.

Western blotting

The cells were rapidly lysed on ice using Blue Loading Buffer Reagents (Cell Signaling Technology, Beverly, MA, USA) containing 0.125 M dithiothreitol. These samples were subjected to 8% SDS-PAGE and were then transferred onto nitrocellulose membranes (Bio-Rad Laboratories, Inc., Hercules, CA, USA). After blocking with 0.1% Tween-added PBS (T-PBS) containing 3% bovine serum albumin (BSA; Sigma-Aldrich), the membranes were incubated with specific primary antibodies against PKCα (Cell Signaling Technology), PKCβ (Abnova Co., Ltd., Taipei, Taiwan), PKCβII (Santa Cruz Biotechnology, Inc., Austin, TX, USA), and β-actin (Sigma-Aldrich). Horseradish peroxidase-conjugated anti-mouse or -rabbit secondary antibody (GE Healthcare, UK) were incubated for 1 h at room temperature in 0.1% T-PBS. The blots were visualized by enhanced chemiluminescence substrate (Thermo Scientific, Rockford, IL, USA) using a Western blotting detection system.

Knockdown of PKCα using RNA interference

MC3T3-E1 cells were transfected with small interfering RNA (siRNA) using Lipofectamine RNAiMAX (Invitrogen) according to the manufacturer's protocol. Two different sets of PKCα siRNA oligos were used for knockdown of PKCα: site 1 (5′-GGAUUUAUCUGAAGGCUGA-3′ and 5′-UCAGCCUUCAGAUAAAUCC-3′) and site 2 (5′-GCAAAGGACUUAUGAC-CAA-3′ and 5′-UUGGUCAUAAGUCCUUUGC-3′) (B-Bridge International, Inc., Sunnyvale, CA, USA). Control siRNA was purchased from B-Bridge International, Inc. MC3T3-E1 cells transfected with siRNA were seeded in a 24-well plate at a concentration of 1.0×10^4 cells/cm^2 for 48 h. The medium was then replaced with differentiation medium and the cells were incubated for 3 days prior to use for experiments.

Infection with adenovirus vectors

Adenovirus expressing rabbit PKCα, rabbit PKCβII, and β-galactosidase were generous gifts from Dr. M. Ohba, Tokyo, Japan [18]. Each recombinant adenovirus was plaque purified, expanded, and titered

Table 1
Sequences of PCR primers and specific probes used for quantitative real-time PCR.

Gene	UPL probe no.	Primer	Sequence (5′→3′)
ALP	81	Forward	ACTCAGGGCAATGAGGTCAC
		Reverse	CACCCGAGTGGTAGTCACAA
Osteocalcin	71	Forward	CACCATGAGGACCCTCTCTC
		Reverse	TGGACATGAAGGCTTTGTCA
Collagen type 1 a1	15	Forward	CATGTTCAGCTTTGTGGACCT
		Reverse	GCAGCTGACTTCAGGGATGT
Runx2	34	Forward	GCCCAGGCGTATTTCAGAT
		Reverse	TGCCTGGCTCTTCTTACTGAG
Osterix	106	Forward	CTCCTGCAGGCAGTCCTC
		Reverse	GGGAAGGGTGGGTAGTCATT
GAPDH	80	Forward	TGTCCGTCGTGGATCTGAC
		Reverse	CCTGCTTCACCACCTTCTTG

Table 2
Sequences of PCR primers used to amplify each of genes in RT-PCR.

Gene	Primer	Sequence (5′→3′)
ALP	Forward	GCCCTCTCCAAGACATATA
	Reverse	CCATGATCACGTCGATATCC
Osteocalcin	Forward	CAAGTCCCACACAGCAGCTT
	Reverse	AAAGCCGAGCTGCCAGAGTT
Collagen type 1 a1	Forward	GCAATCGGGATCAGTACGAA
	Reverse	CTTTCACGCCTTTGAAGCCA
Runx2	Forward	GCTTGATGACTCTAAACCTA
	Reverse	AAAAAGGGCCCAGTTCTGAA
Osterix	Forward	GAAGAAGCTCACTATGGCTC
	Reverse	GAAAAGCCAGTTGCAGACGA
GAPDH	Forward	TGAACGGGAAGCTCACTGG
	Reverse	TCCACCACCCTGTTGCTGTA

in 293 cells (Riken Cell Bank). MC3T3-E1 cells were infected and 2 days later, the medium was replaced with differentiation medium.

Statistical analysis

All data are expressed as means ± SD and a minimum of three independent experiments were performed for each assay. A two-sided unpaired Student's *t*-test, or analysis of variance (ANOVA) for multiple comparisons, was used for statistical analysis. A statistical difference between experimental groups was considered to be significant when the p value was <0.05.

Results

Osteoblastic differentiation of MC3T3-E1 cells is promoted by the PKCα/PKCβI inhibitor Gö6976

Prior to determination of the effects of PKC isoforms on osteoblastic differentiation, we first evaluated the endogenous expression of the PKC isoforms PKCα and PKCβ in MC3T3-E1 cells by western blotting. The expression of PKCα was identified in MC3T3-E1 cells. On the other hand, the expression of PKCβ, which indicates both PKCβI and PKCβII, was almost unidentified in MC3T3-E1 cells (Fig. 1A). We next investigated the effects of the expressed PKCs on osteoblastic differentiation by assay of the effect of incubation of MC3T3-E1 cells with various concentrations of the PKCα/PKCβI inhibitor Gö6976 (0–1.0 μM) for 72 h on ALP staining. In MC3T3-E1 cells, treatment with Gö6976 strongly induced ALP staining in a dose-dependent manner and also enhanced ALP activity (Fig. 1B). Furthermore, Alizarin Red S staining indicated that Gö6976 clearly promoted calcification of the extracellular matrix (ECM) in MC3T3-E1 cells. The degree of this ECM calcification was quantified by measurement of the absorbance of the Alizarin Red S solution (Fig. 1C). Quantitative real-time PCR assay showed acceleration of the mRNA expression of osteoblastic differentiation markers, including ALP, OCN, and Col1a1, and of the transcription factor Runx2, by Gö6976 in a dose-dependent manner (Fig. 1D). These findings indicate that Gö6976 promoted osteoblastic differentiation in MC3T3-E1 cells suggesting that the PKCα and/or PKCβI isoforms might have a suppressive effect on osteoblastic differentiation in MC3T3-E1 cells.

Treatment with the PKCβ inhibitor does not promote osteoblastic differentiation in MC3T3-E1 cells

To investigate which PKC isoform modulates osteoblastic differentiation, we examined the contribution of PKCβ to differentiation using a specific PKCβ inhibitor, which inhibits both PKCβI and PKCβII. Treatment of MC3T3-E1 cells with this PKCβ inhibitor had no influence on ALP activity (Fig. 2A). Moreover, neither calcification of the ECM (Fig. 2B), nor the expression of mRNA related to osteoblastic differentiation (Fig. 2C), changed in the presence of different concentrations of the PKCβ inhibitor. The inhibitor also induced no change in osteoblast-cell proliferation (data not shown). These data indicated that PKCβ, whether it is the PKCβI or PKCβII isoform, did not affect osteoblastic differentiation or cell proliferation. We therefore assumed that inhibition of PKCα by Gö6976 promoted osteoblastic differentiation in MC3T3-E1 cells.

Knockdown of PKCα promotes osteoblastic differentiation

To further confirm the effects of PKCα inhibition on osteoblastic differentiation in MC3T3-E1 cells, we investigated changes in cell differentiation following knockdown of PKCα using an RNA interference method. Fig. 3A shows the low cellular expression level of PKCα, 48 h after transfection of two different anti-PKCα siRNAs (Fig. 3A). Knockdown of PKCα using either siPKCα-1 or siPKCα-2 caused the up-regulation of ALP activity and the acceleration of ECM calcification in MC3T3-E1 cells compared to cells transfected with control siRNA (Figs. 3B and C). Furthermore, quantitative real-time PCR analysis revealed that the gene expression of ALP and OCN was dramatically increased by knockdown of PKCα but not by treatment with control siRNA. Among the other genes tested, the expression of Col1a1 showed some tendency to increase following knockdown of PKCα. Furthermore, knockdown of PKCα increased the mRNA expression of both of the transcription factors Runx2 and Osterix (Figs. 3D, E). These results indicated that PKCα may suppress osteoblastic differentiation.

Activation of PKC by TPA attenuates osteoblastic differentiation in MC3T3-E1 cells

We next investigated the influence of PKC activation by TPA on osteoblastic differentiation. Treatment with TPA (0–10 nM), which activates not only PKCα but also other conventional PKC and novel PKC isoforms, caused a decrease in ALP activity in a dose-dependent manner (Fig. 4A). Activation of PKC by TPA did not stimulate calcification of the ECM in MC3T3-E1 cells (Fig. 4B). In addition, RT-PCR analysis and quantitative real-time PCR showed that the expression of osteoblastic differentiation markers such as ALP and OCN were clearly decreased following TPA treatment in a dose-dependent manner (Figs. 4C, D).

Adenoviral overexpression of PKCα suppresses osteoblastic differentiation in MC3T3-E1 cells

To further confirm the functional role of PKCα in osteoblasts, we performed adenoviral-mediated gene transfer of wild-type PKCα (Ad-PKCα) and PKCβII (Ad-PKCβII) into MC3T3-E1 cells. Following gene transfer, we then confirmed a high expression level of the Ad-PKCα and Ad-PKCβII proteins by western blotting (Fig. 5A). We next measured the proliferation of MC3T3-E1 cells infected with each of the adenovirus vectors Ad-PKCα, Ad-PKCβII or Ad-βgal (control). Compared with cells transfected with Ad-βgal, the proliferation of MC3T3-E1 cells infected with Ad-PKCα was significantly increased on Days 4 and 5 after transfection, while the proliferation of cells transfected with Ad-PKCβII was similar to that of Ad-βgal cells (Fig. 5B). The observed acceleration of the proliferation of Ad-PKCα-transfected MC3T3-E1 cells is consistent with a previous report that PKCα has a stimulatory effect on human osteoblastic proliferation [19]. In addition, the overexpression of PKCα, but not that of PKCβII, suppressed ALP activity compared to overexpression of Ad-βgal (Fig. 5C). Quantitative real-time PCR analysis showed that overexpression of PKCα also suppressed the mRNA expression of ALP, Col1a1, Runx2, and Osterix compared with Ad-βgal (Fig. 5D).

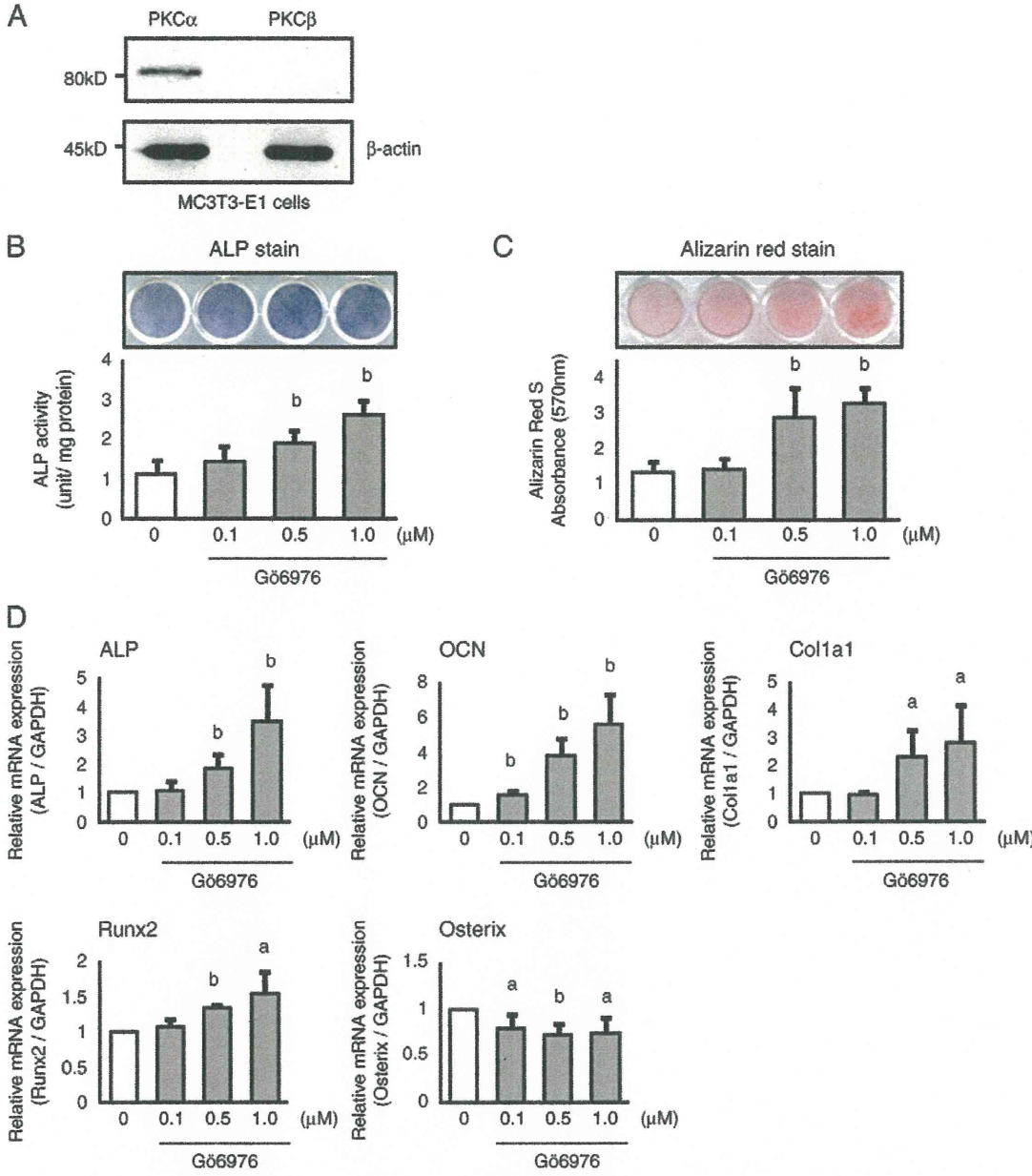

Fig. 1. Osteoblastic differentiation of MC3T3-E1 cells promoted by the PKCα/PKCβI inhibitor Gö6976. (A) endogenous expression of the PKCα, PKCβ proteins in MC3T3-E1 cells by western blotting. β-Actin was used as the internal control. (B) ALP staining and activity of MC3T3-E1 cells treated with Gö6976 which inhibits PKCα and PKCβI. MC3T3-E1 cells (2.0×10^4 cells/cm^2) were cultured in growth medium for 24 h, and then replaced with Gö6976 in differentiation medium for 3 days. (C) MC3T3-E1 cells stained with Alizarin red solution and quantified Ca content in the matrix of the cells. MC3T3-E1 cells were cultured with Gö6976 in differentiation medium for 28 days. Fresh medium was changed twice per week. (D) total RNA isolated from MC3T3-E1 cells treated with Gö6976 for 3 days. mRNA expression of the osteoblast-related genes: *ALP, OCN, Col1α1*; the transcription factor Runx2, and the gene *Osterix* was determined using quantitative real-time PCR analysis and UPL probes. The expression of each gene was normalized to GAPDH expression. (B, C, and D) data are means ± SD of three independent experiments performed in duplicate (a: $p<0.05$, b: $p<0.01$ compared with Gö6976-untreated control).

Discussion

In this study, we showed that PKCα has a suppressive effect on osteoblastic differentiation in MC3T3-E1 cells. Since the PKCα/PKCβI inhibitor Gö6976 accelerated ALP activity, and the PKCβ inhibitor had no influence on ALP activity, we concluded that PKCα is the PKC isoform that functions as a suppressor of osteoblastic differentiation. In addition, we confirmed which isoforms of PKC have specific effects on osteoblastic differentiation in ST2 cells, mouse bone marrow stromal cells. Although ST2 cells are more primitive than MC3T3-E1 cells, they are known to differentiate into osteoblast-like cells in differentiation medium in a similar manner to MC3T3-E1 cells [20]. Treatment of ST2 cells with Gö6976 increased ALP activity, with maximum activity observed at a concentration of 0.5 μM rather than at 1.0 μM, which was the concentration which gave maximum activation in MC3T3-E1 cells. Treatment of ST2 cells with the PKCβ inhibitor or TPA in did not alter ALP activity (data not shown). However, inhibition of PKCα also promoted osteoblastic differentiation in ST2 cells. Taken together, these results suggest that PKCα has a suppressive effect on osteoblastic differentiation that is not cell-type dependent. Thus, we focused on the role of PKCα in osteoblastic differentiation in MC3T3-E1 cells. Knockdown of PKCα promoted osteoblastic differentiation. In addition, calcification of ECM in MC3T3-E1 cells was also accelerated at 28 days after PKCα siRNA

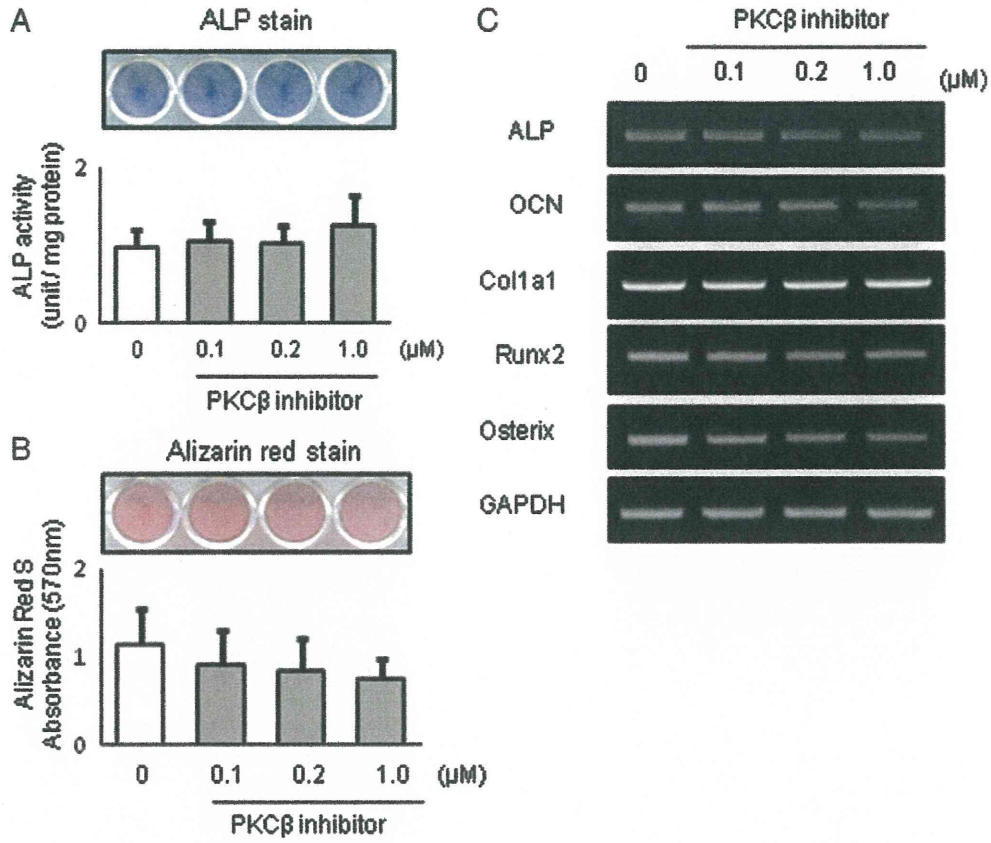

Fig. 2. Effect of PKCβ inhibitor on osteoblastic differentiation in MC3T3-E1 cells. (A) ALP staining and activity of MC3T3-E1 cells. The cells were cultured for 24 h, and then incubated for 3 days with PKCβ inhibitor in differentiation medium. (B) MC3T3-E1 cells stained with Alizarin red solution and quantified Ca content in the matrix of the cells. MC3T3-E1 cells were cultured with PKCβ inhibitor in differentiation medium for 28 days. Fresh medium was changed twice per week. (C) RT-PCR analysis of total RNA isolated from MC3T3-E1 cells treated with PKCβ inhibitor. Expression of osteoblastic related genes: ALP, OCN, Col1α1, Runx2, and Osterix. (A and B) data are means ± SD of three independent experiments performed in duplicate (a: $p<0.05$, b: $p<0.01$ compared with PKCβ inhibitor-untreated control).

transfection (Fig. 3C). In contrast, overexpression of PKCα decreased ALP activity (Fig. 5C) and reduced the expression of the mRNA of osteoblastic markers and transcription factors (Fig. 5D).

PKCα has been implicated in a number of biological functions such as proliferation, differentiation, cell cycle control, apoptosis/cell survival and cell adhesion [21]. In particular, PKCα is known to have an essential role in the proliferation of, not only osteoblasts [19], but also of other normal and tumor cells [22]. In the present study, we further demonstrated that PKCα has a role in the promotion of osteoblastic proliferation (Fig. 5B). Our data are in contrast to two previous reports of the involvement of PKCα in osteoblastic differentiation. Tang et al. [23,24] reported that PKCα is involved in the signal transduction pathway induced by basic fibroblast growth factor (bFGF) during stimulation of fibronectin expression in osteoblasts. The second previous report indicated that fibroblast growth factor receptor 2 (FGFR2) promotes osteogenic differentiation in mesenchymal cells via ERK1/2 and PKCα [25]. In these reports, PKCα was suggested to function in signal transduction pathways that promote osteoblastic differentiation. If PKCα can promote osteoblastic differentiation, inhibition of PKCα by Gö6976 and by PKCα siRNA should decrease osteoblastic differentiation. However, in this study, we showed that inhibition of PKCα promoted osteoblastic differentiation. Since we directly investigated PKCα using an inhibitor of PKCα as well as by knockdown and overexpression of PKCα, our results regarding the role of PKCα in osteoblastic differentiation may be more directly relevant to the cellular role of PKCα. Interestingly, Ogata et al. [26] reported that the G protein, $G\alpha_q$, activated PKC, and subsequently osteoblastic differention was suppressed. Although the isoform of PKC that was involved in the suppression of osteoblastic differentiation was not mentioned in that study, our data suggest the possibility that the results of Ogata might be due to a specific suppressive effect of the PKCα isoform.

Regarding the involvement of other isoforms of PKC in osteoblastic differentiation, there have been some reports that PKCδ activation promotes bone formation [27,28]. We found that treatment of MC3T3-E1 cells with Gö6983, which is an inhibitor of PKCα, β, γ, δ, and ζ, also enhanced ALP activity in a dose-dependent manner (data not shown). To completely rule out the possibility that PKCγ, δ, and ζ may also affect osteoblastic differentiation would require evaluation of the individual roles of PKCγ, δ, or ζ in differentiation. However, our data suggest that it is likely that inhibition of PKCα by Gö6983 strongly contributes to the promotion of ALP activity. Furthermore, PKCα may have a stronger influence on osteoblastic differentiation than PKCδ. Based on the IC_{50} values (half maximal inhibitory concentration) obtained using Gö6983, Gö6983 inhibits PKCα and PKCδ to the same extent [11]. Nevertheless, inhibition of PKCα rather than PKCδ might induce an increase in ALP activity in MC3T3-E1 cells. These results suggest that of the eleven isoforms of PKC, PKCα might have the most important for osteoblastic differentiation. We additionally confirmed that PKCβ, whether it is PKCβI or PKCβII, had little effects on osteoblastic differentiation or cell proliferation. This lack of effect of PKCβ may be related to a lack of expression of PKCβ in osteoblasts, as PKCβ expression has been suggested to be limited to specific tissues such as pancreatic islet cells,monocytes and brain [29]. We suggest that cellular function of PKCα on osteoblasts is not replaced with that of PKCβ, most similar isoform of PKCα.

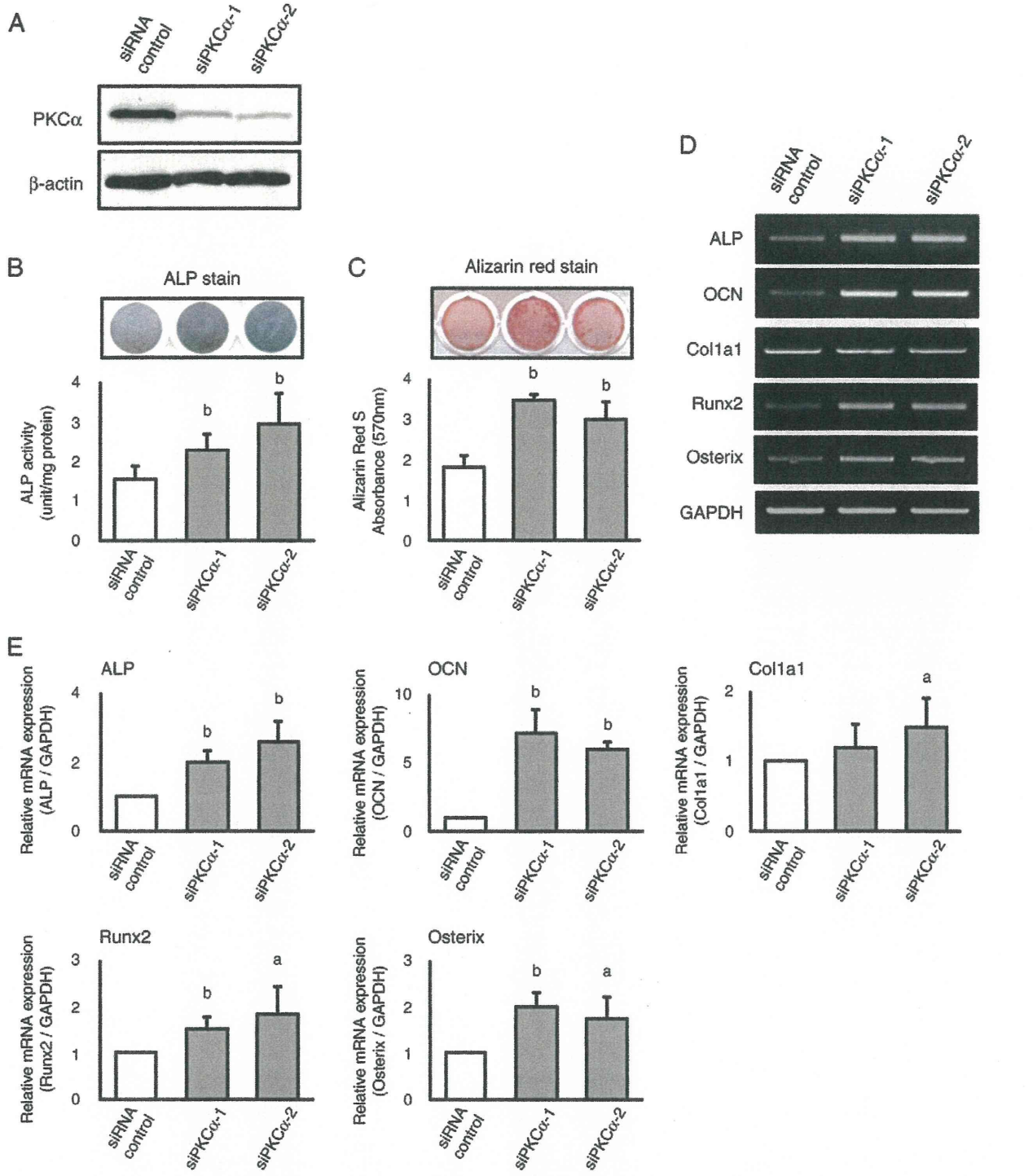

Fig. 3. Knockdown of PKCα stimulates osteoblastic differentiation. (A) Western blotting analysis of PKCα knockdown in MC3T3-E1 cells by transfection with control or PKCα (sites 1 and 2) siRNA. The cells transfected with siRNA were cultured for 48 h. Western blotting was performed using cell lysates as described in Materials and methods. (B) ALP staining and activity of MC3T3-E1 cells transfected with siRNA. The cells transfected with siRNA were incubated for 48 h, following which the medium was changed to differentiation medium. The cells were then incubated for 3 days to evaluate the osteoblastic differentiation. (C) Alizarin red staining and quantified Ca content. MC3T3-E1 cells transfected with control and PKCα siRNA were cultured and incubated in growth medium for 2 days, and then replaced in differentiation medium for 28 days. Fresh medium was changed twice per week. (D and E) expression of osteoblastic-related genes in MC3T3-E1 cells transfected with control and PKCα siRNA was assessed by RT-PCR and quantitative real-time PCR. Total RNA was extracted from MC3T3-E1 cells. The expression of each gene was normalized against GAPDH expression. (B, C, and E) Data are means ± SD of three independent experiments performed in duplicate (a: $p<0.05$, b: $p<0.01$ compared with siRNA control).

Signaling pathways activated downstream of PKCα have been reported to involve the p44/42 MAPK, which is activated by PKCα in various types of cells [19,30–33]. We therefore investigated whether p44/42 MAPK activation is regulated by inhibition of PKCα using the PKC inhibitor or by knockdown of PKCα using RNA interference, or by overexpression of PKCα using Ad-PKCα in MC3T3-E1 cells. However,

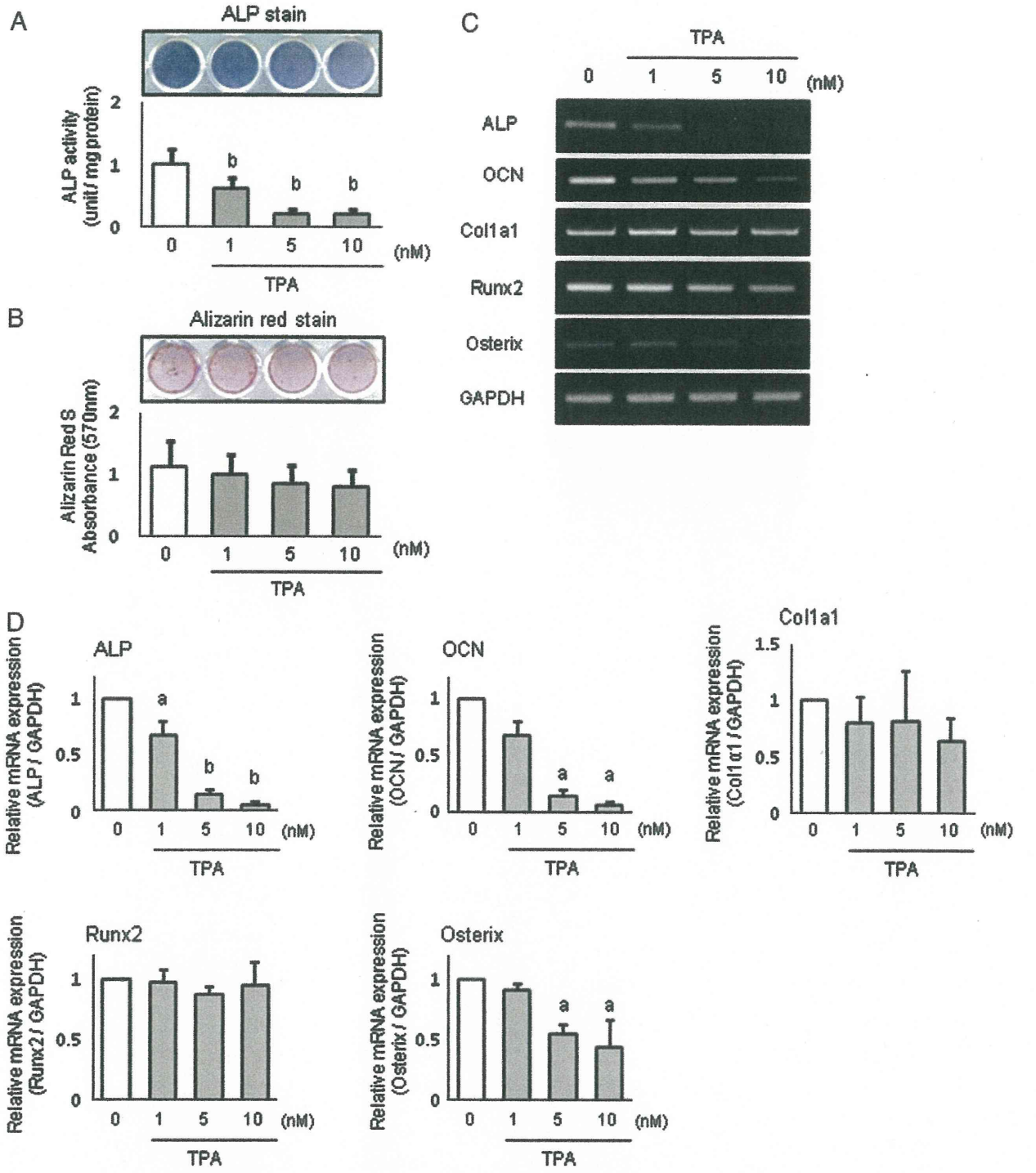

Fig. 4. Effect of TPA on osteoblastic differentiation in MC3T3-E1 cells. (A) ALP staining and activity of MC3T3-E1 cells. The cells were cultured for 24 h, and then incubated for 3 days after treatment with TPA in differentiation medium. (B) MC3T3-E1 cells stained with Alizarin red solution and quantified Ca content in the matrix of the cells. MC3T3-E1 cells were cultured with TPA in differentiation medium for 28 days. Fresh medium was changed twice per week. (C) RT-PCR analysis of total RNA isolated from MC3T3-E1 cells treated with TPA. Expression of osteoblastic-related genes: ALP, OCN, Col1α1, Runx2, and Osterix. (D) total RNA isolated from MC3T3-E1 cells treated with TPA for 3 days. mRNA expression of the osteoblast-related genes: *ALP, OCN, Col1α1*; the transcription factor Runx2, and the gene *Osterix* was determined using quantitative real-time PCR analysis and UPL probes. The expression of each gene was normalized to GAPDH expression. (A, B and D) data are means ± SD of three independent experiments performed in duplicate (a: $p<0.05$, b: $p<0.01$ compared with TPA-untreated control).

significant alteration of the phosphorylation of p44/42 MAPK, as assessed by western blotting, was not correlated with PKCα (data not shown). Interestingly, it is reported that p44/42 MAPK was activated by insulin sitimulation in vastus lateralis skeletal muscles even in a PKCα knockout mouse [34]. Since PKCα plays multiple roles in signal transduction and it does not directly activate p44/42 MAPK [35,36], it is possible that activation of downstream signal pathways other than modulation of p44/42 MAPK by inhibition of PKCα might lead to osteoblastic differentiation. Further study is required to elucidate the signal pathway downstream of PKCα during osteoblastic differentiation.

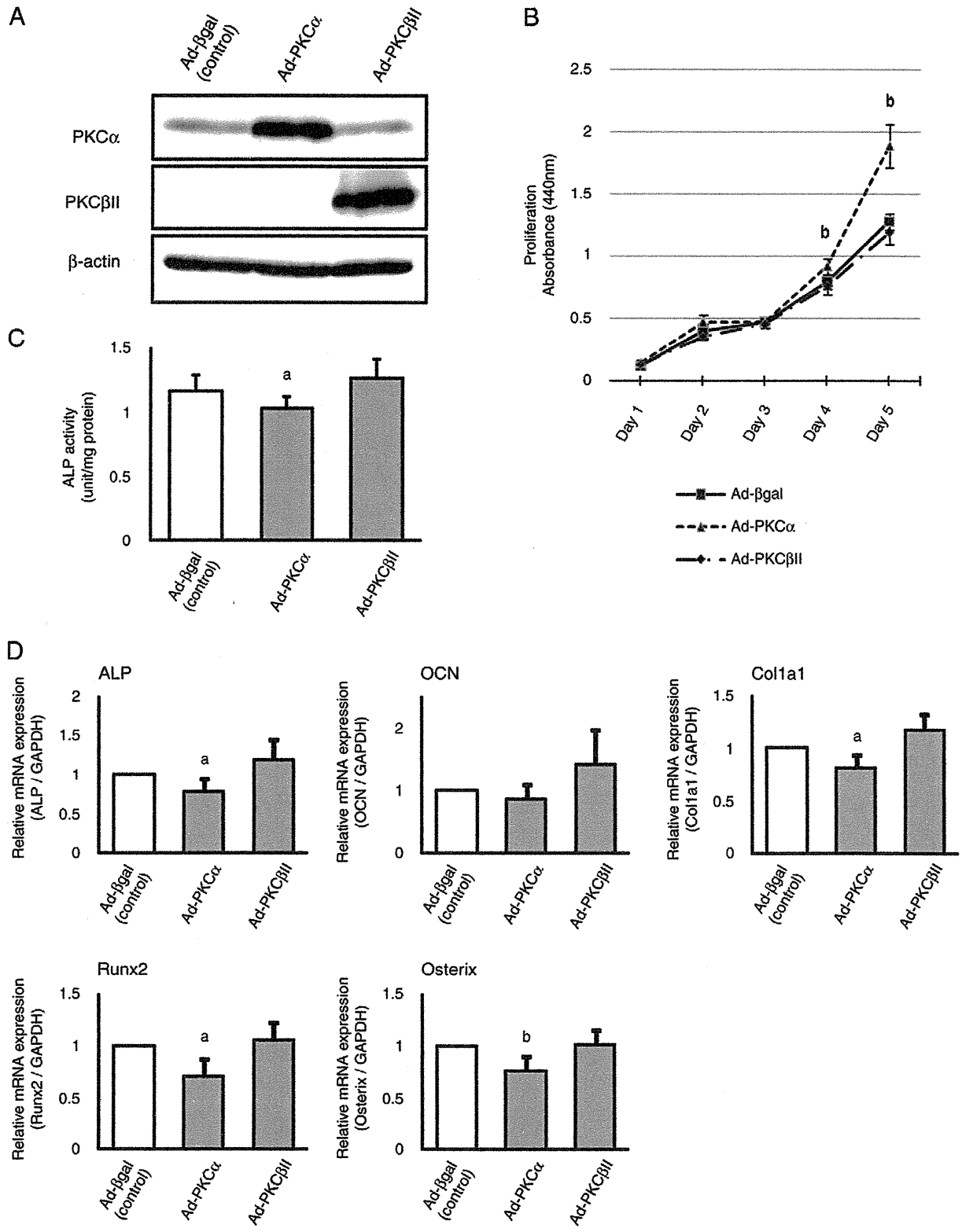

Fig. 5. Effects of PKCα overexpression on MC3T3-E1 cells. (A) Western blotting analysis of PKCα and PKCβII overexpression. Total cell lysates were extracted from MC3T3-E1 cells infected with adenovirus-encoding wild-type of PKCα, PKCβII. (B) proliferation of MC3T3-E1 cells infected with adenovirus encoding an empty vector, (Ad-βgal, control), wild-type PKCα (Ad-PKCα), or PKCβII (Ad-PKCβII). Infected MC3T3-E1 cells were incubated for 2 days following which the medium was changed to differentiation medium and the cells were incubated for a further 3 days. Cell proliferation was assayed at daily intervals over these 5 days of incubation. (C) ALP activity of MC3T3-E1 cells with PKCα overexpression. ALP activity was determined and normalized to the protein content. (D) expression of osteoblastic-related gene in MC3T3-E1 cells infected with Ad-βgal (control), Ad-PKCα, and Ad-PKCβII were assessed by real-time PCR analysis. Total RNA was extracted from MC3T3-E1 cells. (B, C, and D) Data are means ± SD of three independent experiments performed in duplicate (a: $p<0.05$, b: $p<0.01$ compared with Ad-βgal).

In conclusion, the present study indicates that PKCα suppresses osteoblastic differentiation but promoted osteoblastic proliferation. On the other hand, PKCβI and PKCβII had little effect on osteoblastic differentiation or proliferation. In addition, we demonstrated that of the eleven known isoforms of PKC, PKCα is the most important for suppression of osteoblastic differentiation. These results imply that the processes of differentiation and cell proliferation may be different cellular activity, and that PKCα has a pivotal role as a switch between these essential cellular functions.

Acknowledgments

We are grateful to Dr. M. Ohba (Showa University, Tokyo, Japan) for kindly providing the adenovirus expressing rabbit PKCα, rabbit PKCβII, and β-galactosidase. We thank Dr. M. Hirao for scientific advice and for critical reading of the manuscript.

Appendix A. Supplementary data

Supplementary data to this article can be found online at doi:10.1016/j.bone.2010.09.238.

References

[1] Nishizuka Y. The role of protein kinase C in cell surface signal transduction and tumour promotion. Nature 1984;308:693–8.
[2] Nishizuka Y. Turnover of inositol phospholipids and signal transduction. Science 1984;225:1365–70.
[3] Keenan C, Kelleher D. Protein kinase C and the cytoskeleton. Cell Signal 1998;10:225–32.
[4] Lampasso JD, Chen W, Marzec N. The expression profile of PKC isoforms during MC3T3-E1 differentiation. Int J Mol Med 2006;17:1125–31.
[5] Takai Y, Kishimoto A, Inoue M, Nishizuka Y. Studies on a cyclic nucleotide-independent protein kinase and its proenzyme in mammalian tissues: purification and characterization of an active enzyme from bovine cerebellum. J Biol Chem 1977;252:7603–9.
[6] Inoue M, Kishimoto A, Takai Y, Nishizuka Y. Studies on a cyclic nucleotide-independent protein kinase and its proenzyme in mammalian tissues: proenzyme and its activation by calcium-dependent protease from rat brain. J Biol Chem 1977;252:7610–6.
[7] Nishizuka Y. Protein kinase C and lipid signaling for sustained cellular response. FASEB J 1995;9:484–96.
[8] Newton AC. Protein kinase C: Structure, function and regulation. J Biol Chem 1995;270:28495–8.
[9] Boneh A. A model for PKC involvement in the pathogenesis of inborn errors of metabolism. Trends Mol Med 2002;8:524–31.
[10] Martiny-Baron G, Kazanietz MG, Mischak H, Blumberg PM, Kochs G, Hug H, et al. Selective inhibition of protein kinase C isozymes by the indolocarbazole Gö6976. J Biol Chem 1993;268:9194–7.
[11] Gschwendt M, Dieterich S, Rennecke J, Kittstein W, Mueller HJ, Johannes FJ. Inhibition of protein kinase C μ by various inhibitors: differentiation from protein kinase c isoenzymes. FEBS Lett 1996;392:77–80.
[12] Carter CA. Protein kinase C as a drug target: implications for drug or diet prevention and treatment of cancer. Curr Drug Targets 2000;1:163–83.
[13] Teicher BA. Protein kinase C as a theraupic target. Clin Cancer Res 2006;12:5336–45.
[14] Ishii H, Jirousek MR, Koya D, Takagi C, Xia P, Clermont A, et al. Amelioration of vascular dysfunctions in diabetic rats by an oral PKC beta inhibitor. Science 1996;272:728–31.
[15] Tuttle KR, Anderson PW. A novel potential therapy for diabetic nephropathy and vascular complications: protein kinase C beta inhibition. Am J Kidney Dis 2003;42:456–65.
[16] Zini N, Bavelloni A, Lisignoli G, Ghisu S, Valmori A, Martelli AM, et al. PKCζ-expression is lower in osteoblasts from arthritic patients: IL1-β and TNF-α induce a similar decrease in non-arthritic human osteoblasts. J Cell Biolchem 2008;103:547–55.
[17] Cheung WMW, Ng WW, Kung AWC. Dimethyl sulfoxide as an inducer of differentiation in preosteoblast MC3T3-E1 cells. FEBS Lett 2006;580:121–6.
[18] Ohba M, Ishino K, Kashiwagi M, Kawabe S, Chiba K, Huh NH, et al. Induction of differentiation in normal human keratinocytes by adenovirus-mediated introduction of the η and δ isoforms of protein kinase C. Mol Cell Biol 1998;18:5199–207.
[19] Lampasso JD, Marzec N, Margarone J, Dziak R. Role of protein kinase Cα in primary human osteoblastic proliferation. J Bone Miner Res 2002;17:1968–76.
[20] Otsuka E, Yamaguchi A, Hirose S, Hagiwara H. Characterization of osteoblastic differentiation of stromal cell line ST2 that is induced by ascorbic acid. Am J Physiol Cell Physiol 1999;277:132–8.
[21] Michie AM, Nakagawa R. The link between PKCα regulation and cellular transformation. Immunol Lett 2005;96:155–62.
[22] Griner EM, Kazanietz MG. Protein kinase C and other diacylglycerol effectors in cancer. Nat Rev Cancer 2007;7:281–94.
[23] Tang CH, Yang RS, Huang TH, Liu SH, Fu WM. Enhancement of fibronectin fibrillogenesis and bone formation by basic fibroblast growth factor via protein kinase C-dependent pathway in rat osteoblasts. Mol Pharmacol 2004;66:440–9.
[24] Tang CH, Yang RS, Chen YF, Fu WM. Basic fibroblast growth factor stimulates fibronectin expression through phospholipase Cγ, protein kinase Cα, c-Src, NF-κB, and p300 pathway in osteoblasts. J Cell Physiol 2007;211:45–55.
[25] Miraoui H, Oudina K, Petite H, Tanimoto Y, Moriyama K, Marie PJ. Fibroblast growth factor receptor 2 promotes osteogenic differentiation in mesenchymal cells via ERK1/2 and protein kinase C signaling. J Biol Chem 2009;284:4897–904.
[26] Ogata N, Kawaguchi H, Chung UI, Roth SI, Segre G. Continuous activation of $G\alpha_q$ in osteoblasts results in osteopenia through impaired osteoblast differentiation. J Biol Chem 2007;282:35757–64.
[27] Tu X, Joeng KS, Nakayama KI, Nakayama K, Rajagopal J, Carroll TJ, et al. Noncanonical Wnt signaling through G protein-linked PKCδ activation promotes bone formation. Dev Cell 2007;12:113–27.
[28] Kim HJ, Kim JH, Bae SC, Choi JY, Kim HJ, Ryoo HM. The protein kinase C pathway plays a central role in the fibroblast growth factor-stimulated expression and transactivation activity of Runx2. J Biol Chem 2003;278:319–26.
[29] Way KJ, Chou E, King GL. Identification of PKC-isoform-specific biological actions using pharmacological approaches. Trends Pharmacol Sci 2000;21:181–7.
[30] Ansari HR, Teng B, Nadeem A, Roush KP, Martin KH, Schnermann J, et al. A_1 adenosine receptor-mediated PKC and p42/44 MAPK signaling in mouse coronary artery smooth muscle cells. Am J Physiol Heart Circ Physiol 2009;297:1032–9.
[31] Cheng JJ, Wung BS, Chao YJ, Wang DL. Sequential activation of protein kinase C (PKC)-α and PKC-ε sustained Raf/ERK1/2 activation in endothelial cells under mechanical strain. J Biol Chem 2001;276:31368–75.
[32] Braz JC, Bueno OF, De Windt LJ, Molkentin JD. PKCα regulates the hypertrophic growth of cardiomyocytes through extracellular signal-regulated kinase1/2 (ERK1/2). J Cell Biol 2002;156:905–19.
[33] Mauro A, Ciccarelli C, Cesaris PD, Scoglio A, Bouche M, Molinaro M, et al. PKCα-mediated ERK, JNK and p38 activation regulates the myogenic program in human rhabdomyosarcoma cells. J Cell Sci 2002;115:3587–99.
[34] Letiges M, Plomann M, Standaert ML, Bandyopadhyay G, Sajan MP, Kanoh Y, et al. Knockout of PKCα enhances insulin signaling through PI3K. Mol Endcrinol 2002;16:847–58.
[35] Schönwasser DC, Marais RM, Marshall CJ, Parker PJ. Activation of the mitogen-activated protein kinase/extracellular signal-regulated kinase pathway by conventional, novel, and atypical protein kinase C isotypes. Mol Cell Biol 1998;18:790–8.
[36] Johnson GL, Lapadat R. Mitogen-activated protein kinase pathways mediated by ERK, JNK, and p38 protein kinases. Science 2002;298:1911–2.

Biochemical and Biophysical Research Communications 411 (2011) 607–612

Contents lists available at ScienceDirect

Biochemical and Biophysical Research Communications

journal homepage: www.elsevier.com/locate/ybbrc

Induction of chondrogenic cells from dermal fibroblast culture by defined factors does not involve a pluripotent state

Hidetatsu Outani [a,b], Minoru Okada [a,c], Kunihiko Hiramatsu [a,b], Hideki Yoshikawa [b], Noriyuki Tsumaki [a,b,c,d,*]

[a] Department of Bone and Cartilage Biology, Osaka University Graduate School of Medicine, 2-2 Yamadaoka, Suita, Osaka 565-0871, Japan
[b] Department of Orthopaedic Surgery, Osaka University Graduate School of Medicine, 2-2 Yamadaoka, Suita, Osaka 565-0871, Japan
[c] Japan Science and Technology Agency, CREST, Tokyo 102-0075, Japan
[d] Center for iPS Cell Research and Application, Kyoto University, 53 Kawahara-cho, Shogoin, Sakyo-ku, Kyoto 606-8507, Japan

ARTICLE INFO

Article history:
Received 23 June 2011
Available online 6 July 2011

Keywords:
Cartilage
Chondrocytes
Cell reprogramming
Nanog
Pluripotency
iPS cells

ABSTRACT

There is a significant need for cell sources for cartilage regenerative medicine. It has been reported that the combined transduction of two reprogramming factors (c-Myc and Klf4) and one chondrogenic factor (SOX9) directly induces chondrogenic cells from mouse dermal fibroblast (MDF) culture. To gain insights into the process by which cellular characteristics are altered by transduction of c-Myc, Klf4 and SOX9, we examined marker gene expression in the MDF culture at various time points after transduction. The expression of fibroblast-markers was reduced first, followed by an increase in the expression of a chondrocyte-marker. We detected no expression of pluripotent markers at any time point examined. To determine whether or not induced chondrogenic cells go through a pluripotent state after transduction, we analyzed MDFs prepared from Nanog-GFP transgenic mice by monitoring expression of the GFP-labeled pluripotent marker Nanog-GFP in the MDF culture, using time-lapse microscopic observation. Whole-well time-lapse observation revealed that none of the induced chondrogenic cells displayed GFP fluorescence during induction. These results indicate that cells do not undergo a pluripotent state during direct induction of chondrogenic cells from fibroblast culture by transduction of c-Myc, Klf4 and SOX9.

© 2011 Elsevier Inc. All rights reserved.

1. Introduction

Articular hyaline cartilage covers the ends of bones and sustains smooth articulation of joints. Hyaline cartilage consists of chondrocytes that are scattered in an extracellular matrix whose properties define the mechanical function of cartilage. Chondrocytes produce cartilage-specific matrix proteins including types II and XI collagens and aggrecan, and thereby assemble cartilage extracellular matrix. Hyaline cartilage has a very weak capacity for repair. Damage of hyaline cartilage due to trauma or degeneration with age is repaired with fibrous scar tissue which is called fibrocartilage [1]. Fibrocartilage contains type I collagen, which is absent in hyaline cartilage and is inferior in mechanical functions to hyaline cartilage. Fibrocartilage is eventually lost due to mechanical stress, resulting in debilitating conditions, such as osteoarthritis. Currently no drugs have been developed that can induce the production of hyaline cartilage. This means that hyaline cartilage needs to be developed using a regenerative medicine approach. Because chondrocytes are limited in number and their expansion in monolayer culture results in dedifferentiation, as indicated by the expression of type I collagen, there is a significant need for cell sources for cartilage regenerative medicine. Induction of chondrogenic cells from dermal fibroblasts using a cell type conversion technique could increase the supply of a cell source for cartilage regenerative medicine. One such approach is to induce pluripotent stem (iPS) cells from dermal fibroblast culture by transduction of c-Myc, Klf4, Oct3/4, and Sox2 followed by redifferentiation into chondrogenic cells. Although this is a promising approach, it is accompanied by a risk of teratoma formation when the cells are implanted *in vivo*, even after redifferentiation into chondrogenic cells, because a trace of residual pluripotent cells can give rise to teratoma [2]. Recently, a second approach has been reported that involves direct induction of hyaline chondrogenic cells from mouse dermal fibroblast (MDF) culture by transduction of two reprogramming factors (c-Myc and Klf4) and the chondrogenic factor Sox9 [3]. Nonchondrogenic cells in MDF culture give rise to the chondrogenic cells, because the number of prechondrogenic cells indicated by Sox9 expression in MDF culture is much lower than the number of chondrogenic colonies which are induced by transduction of

Abbreviations: MDFs, mouse dermal fibroblasts; iPS cells, induced pluripotent stem cells; *Col1a1*, α1(I) collagen chain gene; *Col1a2*, α2(I) collagen chain gene; *Col2a1*, α1(II) collagen chain gene.

* Corresponding author at: Center for iPS Cell Research and Application, Kyoto University, 53 Kawahara-cho, Shogoin, Sakyo-ku, Kyoto 606-8507, Japan. Fax: +81 6 6879 3798.
E-mail address: ntsumaki@cira.kyoto-u.ac.jp (N. Tsumaki).

0006-291X/$ - see front matter © 2011 Elsevier Inc. All rights reserved.
doi:10.1016/j.bbrc.2011.06.194

c-Myc, Klf4, and SOX9 [3]. This technique of direct conversion appears simpler than the approach that involves iPS cells and can therefore shorten the putative reprogramming process. The resulting reduction in excessive reprogramming is likely to contribute to the safety of the induced cells, including reduced genomic aberrations and reduced risk of teratoma formation when implanted *in vivo*. However, it is not clear whether chondrogenic cells induced by this technique that employs c-Myc and Klf4 have, in actuality, not gone through a pluripotent state during the process by which fibroblasts are reprogrammed into chondrogenic cells.

To examine the effects of transduction of c-Myc, Klf4, and SOX9 on the characteristics of MDFs, we analyzed the mRNA expression of pluripotent markers by MDFs over several days after transduction of c-Myc, Klf4 and SOX9 using RT-PCR. Pluripotent markers, including Nanog and Oct3/4, were not expressed. We then analyzed MDFs prepared from Nanog-GFP transgenic mice [4], using real-time monitoring of pluripotent markers. Time-lapse full-scan observation of cells in culture dishes showed that the cells that later became chondrogenic cells exhibited only background levels of Nanog-GFP fluorescence. These results indicate that chondrogenic cells are induced from mouse fibroblast culture without going through a pluripotent state.

2. Materials and methods

2.1. Preparation of Nanog-GFP MDFs

For MDF isolation, skin was prepared from six-week-old Nanog-GFP transgenic mice [4]. After the hair was shaved off, the skin was minced and trypsinized at 37 °C for 4 h. Dissociated cells were filtered through a nylon mesh (pore size, 40 μm; Tokyo Screen, Tokyo, Japan) to generate a single-cell suspension and then seeded onto 100 mm dishes and cultured in DMEM supplemented with 10% FBS (passage 1).

2.2. Retroviral transduction and time-lapse imaging

Retroviral infection was performed as described previously [5]. One day after seeding Plat-E cells [6] at a density of 3.6×10^6 cells per 10 cm dish, we transfected the cells with pMXs-c-Myc (Addgene plasmid 13375), pMXs-Klf4 (Addgene plasmid 13370), pMXs-Oct3/4 (Addgene plasmid 13366), pMXs-Sox2 (Addgene plasmid 13367) [5], and pMXs-hSOX9 by using the Fugene 6 transfection reagent (Roche). Twenty-four hours after transfection, the medium was replaced. Twenty-four hours after medium replacement, the medium was collected as the virus-containing supernatant from Plat-E cultures.

Frozen stored MDFs were thawed, seeded onto 100 mm dishes and cultured in DMEM supplemented with 10% FBS. One day before transduction, the cells were trypsinized and replated at a density of 1.7×10^5 cells per 6 cm dish (passage 3).

The virus-containing supernatants were filtered through a 0.45 μm cellulose acetate filter (Schleicher & Schuell) and were supplemented with 4 μg/ml polybrene (Nacalai Tesque).

Equal amounts of supernatants containing each of the retroviruses (pMXs-c-Myc, pMXs-Klf4, and pMXs-SOX9 for induction of chondrogenic cells; pMXs-c-Myc, pMXs-Klf4, pMXs-Oct3/4, and pMXs-Sox2 for induction of iPS cells) were mixed and added to the MDF cultures (day 0). After overnight (16 h) incubation in the virus-containing medium, the fibroblast culture in the 6 cm dish was trypsinized and replated into six wells of a six-well plate in fresh medium (day 1). The plates were subjected to time-lapse GFP observation using Biostation CT (Nikon). Phase and GFP images were captured every 8 h for 20 consecutive days. Entire wells were each scanned using a total of 64 images (8 rows × 8 columns), and a tiled image was reconstituted. Each image in the movie is shown for 0.5 s, thus 8 h corresponds to 0.5 s. For induction of chondrogenic cells the DMEM medium supplemented with 10% FBS was changed every other day. On day 21, the cells in the dishes were stained with toluidine blue. For induction of iPS cells, the cells were replated on SNL feeder cells at a density of 2×10^4 cells per well in a six-well plate and the medium was changed to ES cell medium the next day according to a previously described method [7].

2.3. Real-time RT-PCR and RT-PCR analyses

RNA was extracted from the MDF cells in culture just before (day 0), and various days after transduction with c-Myc, Klf4, and SOX9 by using RNeasy Mini Kits (Qiagen). Total RNA was digested with DNase to eliminate any contaminating genomic DNA. For real-time quantitative RT-PCR, 1 μg of total RNA was reverse transcribed into first-strand cDNA by using SuperScript III (Invitrogen) and an oligo$(dT)_{20}$ primer. The PCR amplification was performed in a reaction volume of 20 μl containing 2 μl of cDNA, 10 μl of SYBER PremixExTaq (Takara) and 7900HT (Applied Biosystems). The RNA expression levels were normalized to the level of *Gapdh* expression. For RT-PCR analysis, 1 μg of total RNA was reverse transcribed into first-strand cDNA by using SuperScript III (Invitrogen) and oligo$(dT)_{20}$ primers. PCR was performed using the KODFX DNA polymerase (Toyobo). The primers used are listed in Table 1. Control cells that were similarly analyzed were E14tg2a ES cells that were maintained as described previously [8] and the differentiated iPS cells *d-iPS1* and *2* [7].

2.4. Immunohistochemistry

After retroviral transduction of MDFs with c-Myc, Klf4, and Sox9, the cultures were continued for 3 weeks. Following fixation with 4% paraformaldehyde, nodules were picked-up manually, transferred into gelatin, and processed for sectioning for histologic analysis. Immunohistochemical analysis was performed using anti-type II collagen antibody (Thermo #MS-235-P0, dilution

Table 1
Sequences of the PCR primers used.

Primer	Sequence
Col1a1 S	GCAACAGTCGCTTCACCTAC
Col1a1 AS	GTGGGAGGGAACCAGATTG
Col1a2 S	TCGGGCCTGCTGGTGTTCGTG
Col1a2 AS	TGGGCGCGGCTGTATGAGTTCTTC
Col2a1 S	TTGAGACAGCACGACGTGGAG
Col2a1 AS	AGCCAGGTTGCCATCGCCATA
Gapdh S	GAGATGATGACCCTTTTGGCT
Gapdh AS	TCAAGGCCGAGAATGGGAAG
Nanog S	TCTTCCTGGTCCCCACAGTTT
Nanog AS	GCAAGAATAGTTCTCGGGATGAA
Oct3/4 S	CTGAGGGCCAGGCAGGAGCACGAG
Oct3/4 AS	CTGTAGGGAGGGCTTCGGGCACTT
Sox2 S	GGTTACCTCTTCCTCCCACTCCAG
Sox2 AS	TCACATGTGCGACAGGGGCAG
Rex1 S	ACGAGTGGCAGTTTCTTCTTGGGA
Rex1 AS	TATGACTCACTTCCAGGGGGCACT
Utf1 S	GGATGTCCCGGTGACTACGTCTG
Utf1 AS	GGCGGATCTGGTTATCGAAGGGT
Brachyury S	AACTTTCCTCCATGTGCTGAGAC
Brachyury AS	TGACTTCCCAACACAAAAAGCT
Mixl1 S	ACTTTCCAGCTCTTTCAAGAGCC
Mixl1 AS	ATTGTGTACTCCCCAACTTTCCC
Afp S	TGCAGAAACACATCGAGGAGAG
Afp AS	GCTTCACCAGGTTAATGAGAAGC
Sox17 S	TTTGTGTATAAGCCCGAGATGG
Sox17 AS	AAGATTGAGAAAACACGCATGAC

1:200) and anti-Aggrecan antibodies (Santa Cruz, sc-25674, dilution 1:200). Immune complexes were detected using Alexa Fluor 488 (Invitrogen). DNA was stained with Hoechst 33,342 (invitrogen H3570).

All experiments were approved by our institutional animal committee (the Institutional Animal Care and Use Committee (IACUC) of Osaka University Graduate School of Medicine) and institutional biosafety committee (Osaka University Living Modified Organism (LMO) Experiments Safety Committee).

3. Results

3.1. Analysis of fibroblast- and chondrocyte-marker gene expression by MDFs after transduction of c-Myc, Klf4 and SOX9

To gain some insight into the course of the alteration in cell characteristics following transduction of c-Myc, Klf4 and SOX9 into MDFs, we analyzed MDF expression of fibroblast- and chondrocyte-marker genes over several days after transduction, using real-time RT-PCR analysis of MDF RNA (Fig. 1A). The mRNA expression levels of the fibroblast-markers, α1(I) collagen chain gene (*Col1a1*) and α2(I) collagen chain gene (*Col1a2*), were maintained for 1 day after transduction but were reduced 2 days after transduction. On the other hand, the expression level of the chondrocyte-marker gene, α1(II) collagen chain gene (*Col2a1*), was substantially increased on day 5 after transduction. These results suggest that transduction of c-Myc, Klf4 and SOX9 into MDFs decreases fibroblastic characteristics, and this decrease is then followed by acquisition of a chondrogenic phenotype. To confirm that chondrogenic cells were indeed induced in this culture system as previously reported [3], we continued the culture for 3 weeks after transduction and then stained the cells using cartilage-specific stains. Cell aggregates with a nodular appearance were formed in the dishes and displayed metachromatic toluidine blue staining

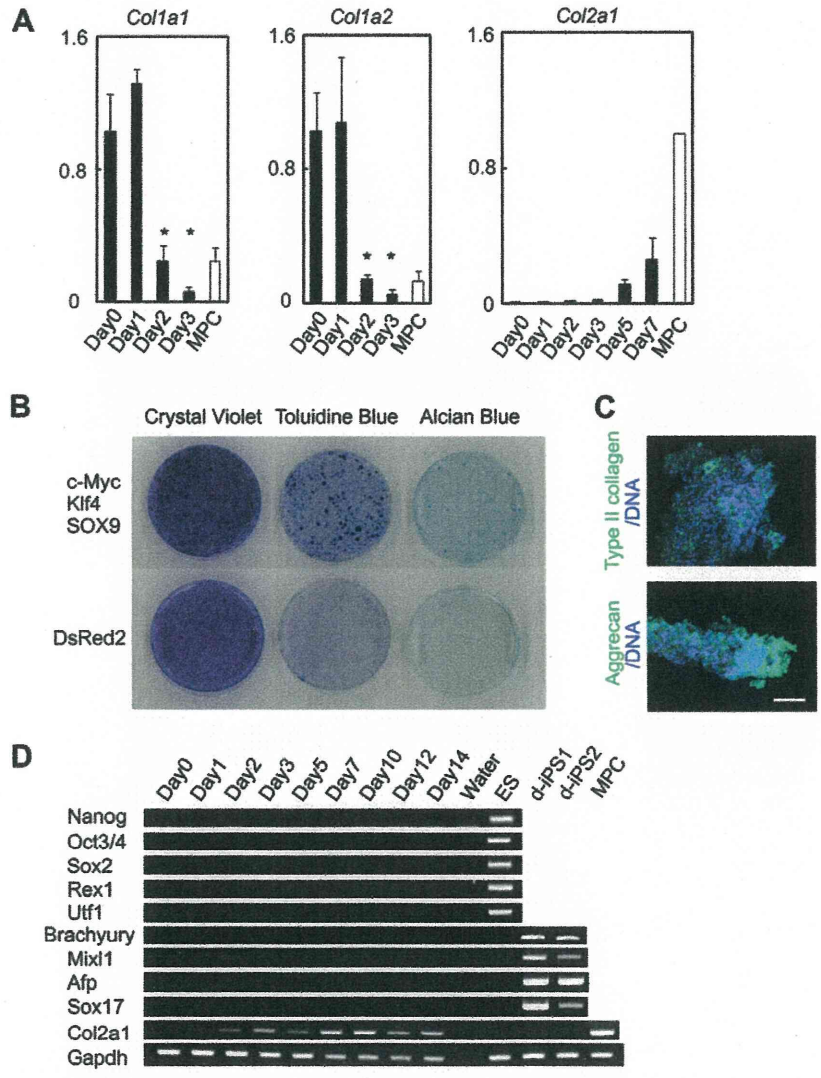

Fig. 1. Analysis of marker gene expression in MDFs after transduction of c-Myc, Klf4 and SOX9. RNA was collected at the time points indicated at the bottom of each graph. (A) Real-time RT-PCR analysis of the mRNA expression of fibroblast- and chondrocyte-marker genes. *MPC*, mouse primary chondrocytes. Error bars indicate mean ± SD ($n = 3$). For *Col1a1* and *Col1a2*, $^*p < 0.05$ between samples on day 0 and samples collected at each time point as determined using Student's *t* test. (B) MDF culture dishes stained with crystal violet, toluidine blue or alcian blue 21 days after transduction of c-Myc, Klf4 and SOX9, or DsRed2. (C) Nodules that had formed in the MDF culture dishes 21 days after transduction of c-Myc, Klf4 and SOX9 were picked-up, sectioned and immunostained with anti-type II collagen antibodies (green) and anti-Aggrecan antibodies (green). DNA was stained with Hoechst 33,342 (blue). Scale bar, 100 μm. (D) RT-PCR analysis of the mRNA expression of pluripotent- and developmental-marker genes. *ES*, E14tg2a embryonic stem cells; *d-iPS1* and *2*, differentiated iPS cells; *MPC*, mouse primary chondrocytes.

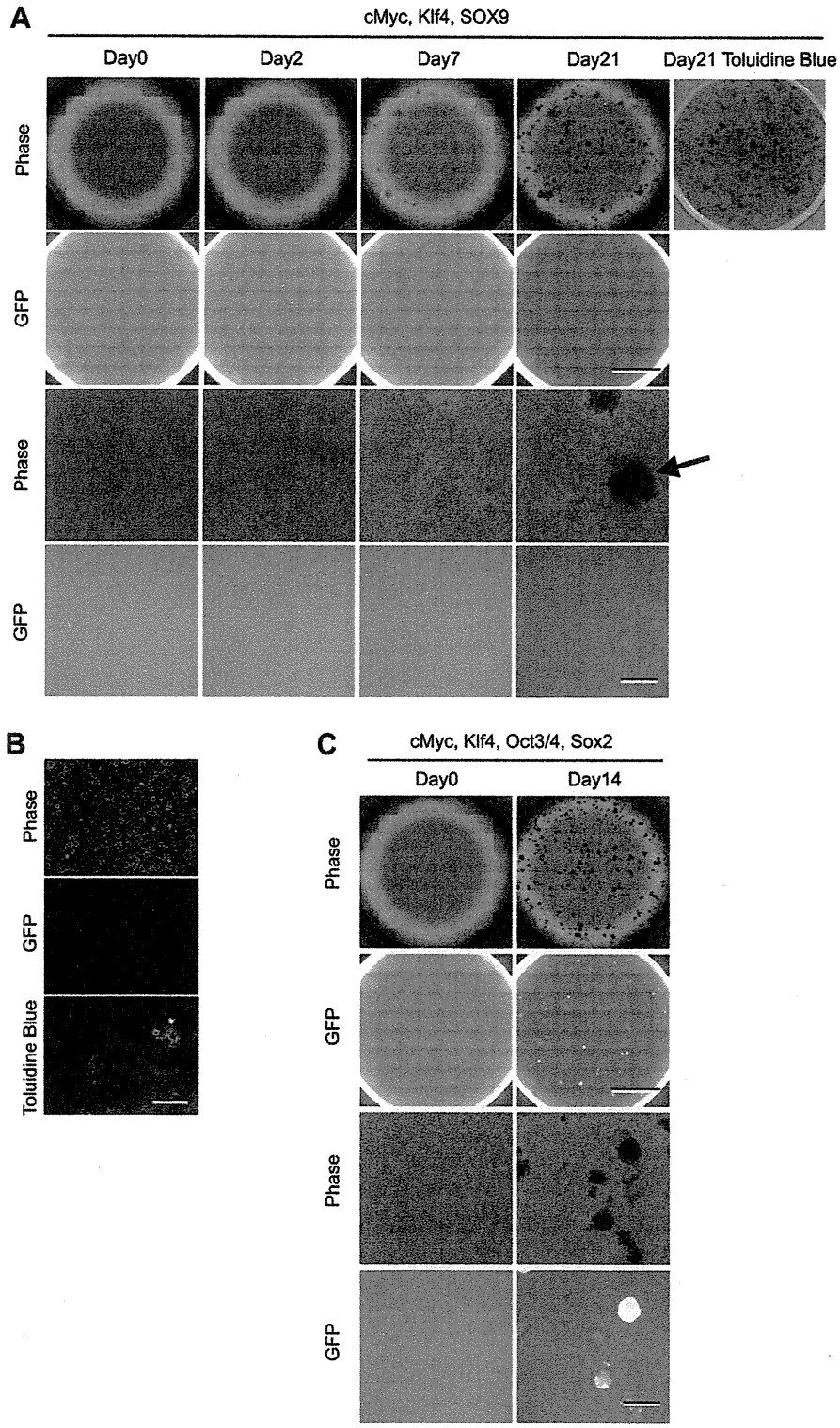

Fig. 2. Time-lapse images of Nanog-GFP MDF culture transduced with c-Myc, Klf4 and SOX9. (A) Time-lapse phase contrast (top row) and GFP fluorescence (second row) tiled images, spanning an entire well of a six-well plate. The top right panel shows toluidine blue staining of the well whose phase image is shown at left. One magnified phase (third row) and GFP fluorescent (bottom row) image is shown. Scale bars: 10 mm in top and second rows; 1 mm in third and bottom rows. (B) Magnification of the nodules indicated by an *arrow* in the right panel in the third row in (A). Scale bar, 100 μm. (C) As a control, Nanog-GFP MDFs were transduced with c-Myc, Klf4, Oct3/4 and Sox2. Phase contrast (top row) and GFP fluorescent (second row) tiled images, spanning an entire well of a six-well plate are shown. One magnified phase contrast (third row) and GFP fluorescent (bottom) image is shown. Scale bars: 10 mm in top and second rows; 1 mm in third and bottom rows (For interpretation of the references to color in this figure legend, the reader is referred to the web version of this article).

and intense Alcian blue staining (Fig. 1B). In addition, immunohistochemical analysis detected type II collagen and Aggrecan immunoreactivity in the nodules (Fig. 1C). These results suggested that chondrogenic cells were induced and formed cartilaginous nodules following transduction.

3.2. Analysis of pluripotent- and developmental-maker gene expression in MDFs after transduction of c-Myc, Klf4 and SOX9

We next examined the expression of pluripotent markers in the MDFs over a period of 14 days after transduction of c-Myc, Klf4 and SOX9, using RT-PCR. Expression of *Nanog*, *Oct3/4*, *Sox2*, *Rex1*, and *Utf1* mRNA were all below the detectable level over the time-course examined, whereas their expression was detected in Embryonic Stem (ES) cells (Fig. 1D). Analysis of the expression of markers of specific developmental stages could not detect expression of genes characteristic of early mesoderm (Brachyury and Mixl1) or of early endoderm (Afp and Sox17) (Fig. 1D). These results suggest that transduction of c-Myc, Klf4 and SOX9 do not guide MDFs to these specific early developmental pathways.

3.3. Time-lapse observation of Nanog-GFP fluorescence during induction of chondrogenic cells

A small number of the cells in the MDF culture that were transduced with c-Myc, Klf4 and SOX9 gave rise to chondrogenic cells in the culture dishes (Fig. 1B) [3]. The majority of the cells appeared as fast-proliferating types of fibroblasts that were transduced with the factors but were not guided to the chondrogenic lineage. To determine whether the induced chondrogenic cells go through a pluripotent stem cell state or not, we monitored pluripotency at the single cell level by using MDFs prepared from Nanog-GFP transgenic mice. Nanog-GFP transgenic mice bear the BAC transgene in which EGFP is inserted into the 5′-untranslated region of the Nanog gene, and express GFP in a pattern that is identical to that of Nanog [4]. To detect potential transient expression of Nanog-GFP, we monitored Nanog-GFP fluorescence at 8 h intervals. An entire well of a six-well plate was analyzed using 64 images (8 rows × 8 columns). To construct a whole-well view, these 64 images were tiled for each well. The time-lapse tiled phase contrast image, which spanned an entire well of a six-well plate, indicated that multiple nodules appeared at 7 days after transduction of c-Myc, Klf4 and SOX9 into Nanog-GFP MDFs (Fig. 2A, top row; Movie S1). These nodules gradually grew in size. Toluidine blue staining showed metachromatic staining of the nodules at 21 days after transduction (Fig. 2A, top right panel), suggesting that these nodule contain glycosaminoglycan and are therefore chondrogenic. Analysis of GFP fluorescence showed background levels of fluorescence throughout the observation period (Fig. 2A, second row; Movie S2). Detailed examination of each image revealed that cells proliferated vigorously on day 2 and started to form nodules by day 7 (Fig. 2A, third row; Movie S3), which is consistent with a previous report [3]. The nodules had become substantial in size by 21 days after transduction (Fig. 2A third right panel). Each nodule was composed of multilayered polygonal-shaped cells and showed metachromatic toluidine blue staining (Fig. 2B), indicating that these cells were chondrogenic. A total of six wells were analyzed in this manner, in which 64 phase contrast and GFP-fluorescent images were captured per well, 3 times a day (8 h intervals), for 20 days. Thus, 23,040 phase contrast and GFP images were captured in total. Nanog-GFP fluorescence was at background levels in all cells, in all 23,040 GFP images, including cells which were later shown to become chondrogenic cells (Table 2; Fig. 2A, bottom; Movie S4). In contrast, the control iPS cells used for this study showed intense GFP fluorescence following transduction of c-Myc, Klf4, Oct3/4 and Sox2 (Fig. 2C; Movies S5–8). Substantial GFP fluorescence was detected as early as 8–9 days after transduction (Movies S6 and S8).

Table 2
Number of nodules showing metachromatic toluidine blue staining and number of cells showing Nanog-GFP fluorescence after transduction of c-Myc, Klf4 and SOX9.

Well of a six-well plate	Number of cells seeded	Number of nodules with metachromatic toluidine blue staining	Number of cells with GFP fluorescence[a]
1	5.1×10^4	20	0
2	5.1×10^4	65	0
3	5.1×10^4	25	0
4	2.5×10^4	12	0
5	2.5×10^4	15	0
6	2.5×10^4	15	0
Total	2.3×10^5	152	0

[a] Sum of numbers of cells showing GFP fluorescence throughout observation.

4. Discussion

4.1. Cells do not pass through a pluripotent state during chondrogenic induction

We did not detect mRNA expression of pluripotent stem cell markers including *Nanog*, *Oct3/4*, *Sox2*, *Rex1*, and *Utf1* in cells over a period of 14 days after transduction of c-Myc, Klf4, and SOX9, using RT-PCR analysis. We also did not detect Nanog-GFP expression above background levels in any of the cultured cells using time-lapse analysis. Based on these results, we concluded that cells do not pass through a pluripotent state during direct induction of chondrogenic cells from fibroblast culture. It has been shown that *in vivo* transplantation of chondrogenic cells that were directly induced from dermal fibroblasts in culture does not result in the production of a teratoma [3]. Our results confirmed that, at least in theory, these induced chondrogenic cells should not produce a teratoma when implanted *in vivo*.

The generation of iPS cells is associated with vigorous epigenetic reprogramming, which can possibly cause DNA damage and genomic instability [9,10]. If the degree of nuclear reorganization during the cell reprogramming process is lower during direct induction of chondrogenic cells from fibroblasts than that during induction through iPS cells, then it is possible that genomic aberrations will also be reduced in the directly induced chondrogenic cells compared with those which are induced through iPS cells.

The sensitivity of detection of GFP fluorescence in our experiment was high, since we were able to detect Nanog-GFP fluorescence during induction of iPS cells as early as day 8–9. We therefore concluded that Nanog-GFP was not expressed by any cell during induction of chondrogenic cells. However, it is still formally possible that we may have missed a very short-lived, transient expression of Nanog-GFP, if the GFP proteins were rapidly degraded in cells during chondrogenic cell induction.

Although efficient induction of iPS cells requires transduction of four reprogramming factors, it has been reported that transduction of three factors (Klf4, Oct3/4, Sox2) can reprogram fibroblasts into iPS cells with low efficiency [11]. Furthermore, transduction of neural stem cells with Oct3/4 alone [12], transduction of certain somatic cells with Oct3/4 in combination with specific chemical molecules [13], or transduction of follicle dermal papilla cells with Oct3/4 alone [14] results in the induction of iPS cells. These findings imply that transduction of fewer reprogramming factors could produce a pluripotent stem cell state, if the appropriate cells or conditions are used. However, the efficiency of iPS cell induction is very low when the number of reprogramming factors is reduced, compared with the 0.1% efficiency of induction of chondrogenic

cells from dermal fibroblast culture [3]. These findings support the notion that cells do not undergo a pluripotent stem cell state during induction of chondrogenic cells from dermal fibroblast culture by transduction of c-Myc, Klf4 and SOX9.

4.2. Sequence of the disappearance of fibroblastic characteristics and chondrogenic commitment

It has been reported that, during induction of iPS cells by forced expression of c-Myc, Klf4, Oct3/4 and Sox2, downregulation of the fibroblast-marker Thy1 occurs first, which is then followed by upregulation of pluripotent markers [15]. Transduction of a combination of c-Myc and Klf4 is the most effective for downregulation of a fibroblast marker, suggesting that c-Myc and Klf4 are responsible for the disappearance of fibroblastic characteristics [16]. In the present study, marked downregulation of *Col1a1* and *Col1a2* mRNA expression began on day 2, and was followed by a gradual upregulation of Col2a1 mRNA expression between days 5–7 after transduction of c-Myc, Klf4, and SOX9. Combined with previous data, it is likely that elimination of the fibroblastic phenotype is induced by c-Myc and Klf4. Commitment and differentiation into chondrogenic cells, which is caused by SOX9, appears to take place once the fibroblast phenotype is eliminated.

In summary, our results indicate that chondrogenic cells induced by c-Myc, Klf4 and SOX9 from MDFs do not pass through a pluripotent state during induction. Such directly induced chondrogenic cells may be safer than chondrogenic cells that were redifferentiated from iPS cells in terms of the risks of teratoma formation and genomic aberrations.

Acknowledgments

We thank Shinya Yamanaka for providing the Nanog-GFP mice and the retroviral vectors. We also thank Toshio Kitamura for the Plat-E cells and the pMX retroviral vectors and Yoshihiro Yoneda for the *d-iPS1* and *2* cells. This study was supported in part by JST, CREST and Scientific Research Grant No. 21390421 from MEXT.

Appendix A. Supplementary data

Supplementary data associated with this article can be found, in the online version, at doi:10.1016/j.bbrc.2011.06.194.

References

[1] A. Bedi, B.T. Feeley, R.J. Williams 3rd, Management of articular cartilage defects of the knee, J. Bone Joint Surg. Am. 92 (2010) 994–1009.
[2] M. Wernig, J.P. Zhao, J. Pruszak, E. Hedlund, D. Fu, F. Soldner, V. Broccoli, M. Constantine-Paton, O. Isacson, R. Jaenisch, Neurons derived from reprogrammed fibroblasts functionally integrate into the fetal brain and improve symptoms of rats with Parkinson's disease, Proc. Natl. Acad. Sci. U S A 105 (2008) 5856–5861.
[3] K. Hiramatsu, S. Sasagawa, H. Outani, K. Nakagawa, H. Yoshikawa, N. Tsumaki, Generation of hyaline cartilaginous tissue from mouse adult dermal fibroblast culture by defined factors, J. Clin. Invest. 121 (2011) 640–657.
[4] K. Okita, T. Ichisaka, S. Yamanaka, Generation of germline-competent induced pluripotent stem cells, Nature 448 (2007) 313–317.
[5] K. Takahashi, S. Yamanaka, Induction of pluripotent stem cells from mouse embryonic and adult fibroblast cultures by defined factors, Cell 126 (2006) 663–676.
[6] S. Morita, T. Kojima, T. Kitamura, Plat-E: an efficient and stable system for transient packaging of retroviruses, Gene Ther. 7 (2000) 1063–1066.
[7] M. Okada, Y. Yoneda, The timing of retroviral silencing correlates with the quality of induced pluripotent stem cell lines, Biochim. Biophys. Acta 1810 (2010) 226–235.
[8] H. Niwa, T. Burdon, I. Chambers, A. Smith, Self-renewal of pluripotent embryonic stem cells is mediated via activation of STAT3, Genes Dev. 12 (1998) 2048–2060.
[9] Y. Mayshar, U. Ben-David, N. Lavon, J.C. Biancotti, B. Yakir, A.T. Clark, K. Plath, W.E. Lowry, N. Benvenisty, Identification and classification of chromosomal aberrations in human induced pluripotent stem cells, Cell Stem Cell 7 (2010) 521–531.
[10] S.M. Hussein, N.N. Batada, S. Vuoristo, R.W. Ching, R. Autio, E. Narva, S. Ng, M. Sourour, R. Hamalainen, C. Olsson, K. Lundin, M. Mikkola, R. Trokovic, M. Peitz, O. Brustle, D.P. Bazett-Jones, K. Alitalo, R. Lahesmaa, A. Nagy, T. Otonkoski, Copy number variation and selection during reprogramming to pluripotency, Nature 471 (2011) 58–62.
[11] M. Nakagawa, M. Koyanagi, K. Tanabe, K. Takahashi, T. Ichisaka, T. Aoi, K. Okita, Y. Mochiduki, N. Takizawa, S. Yamanaka, Generation of induced pluripotent stem cells without Myc from mouse and human fibroblasts, Nat. Biotechnol. 26 (2008) 101–106.
[12] J.B. Kim, V. Sebastiano, G. Wu, M.J. Arauzo-Bravo, P. Sasse, L. Gentile, K. Ko, D. Ruau, M. Ehrich, D. van den Boom, J. Meyer, K. Hubner, C. Bernemann, C. Ortmeier, M. Zenke, B.K. Fleischmann, H. Zaehres, H.R. Scholer, Oct4-induced pluripotency in adult neural stem cells, Cell 136 (2009) 411–419.
[13] S. Zhu, W. Li, H. Zhou, W. Wei, R. Ambasudhan, T. Lin, J. Kim, K. Zhang, S. Ding, Reprogramming of human primary somatic cells by OCT4 and chemical compounds, Cell Stem Cell 7 (2010) 651–655.
[14] S.Y. Tsai, B.A. Bouwman, Y.S. Ang, S.J. Kim, D.F. Lee, I.R. Lemischka, M. Rendl, Single transcription factor reprogramming of hair follicle dermal papilla cells to induced pluripotent stem cells, Stem cells 29 (2011) 964–971.
[15] M. Stadtfeld, N. Maherali, D.T. Breault, K. Hochedlinger, Defining molecular cornerstones during fibroblast to iPS cell reprogramming in mouse, Cell Stem Cell 2 (2008) 230–240.
[16] R. Sridharan, J. Tchieu, M.J. Mason, R. Yachechko, E. Kuoy, S. Horvath, Q. Zhou, K. Plath, Role of the murine reprogramming factors in the induction of pluripotency, Cell 136 (2009) 364–377.

THE JOURNAL OF BIOLOGICAL CHEMISTRY VOL. 286, NO. 4, pp. 3094–3103, January 28, 2011
© 2011 by The American Society for Biochemistry and Molecular Biology, Inc. Printed in the U.S.A.

Cellular ATP Synthesis Mediated by Type III Sodium-dependent Phosphate Transporter *Pit-1* Is Critical to Chondrogenesis*

Received for publication, May 25, 2010, and in revised form, October 13, 2010 Published, JBC Papers in Press, November 12, 2010, DOI 10.1074/jbc.M110.148403

Atsushi Sugita[‡§], Shinji Kawai[¶], Tetsuyuki Hayashibara[‖], Atsuo Amano[¶], Takashi Ooshima[‖], Toshimi Michigami[**], Hideki Yoshikawa[§], and Toshiyuki Yoneda[‡1]

From the Departments of [‡]Biochemistry, [¶]Oral Frontier Biology, and [‖]Pediatric Dentistry, Osaka University Graduate School of Dentistry, and the [**]Department of Bone and Mineral Research, Osaka Medical Center and Research Institute for Maternal and Child Health, Izumi, Osaka 594-1101, Japan and the [§]Department of Orthopaedic Surgery, Osaka University Graduate School of Medicine, Suita, Osaka 565-0871, Japan

Disturbed endochondral ossification in X-linked hypophosphatemia indicates an involvement of P_i in chondrogenesis. We studied the role of the sodium-dependent P_i cotransporters (NPT), which are a widely recognized regulator of cellular P_i homeostasis, and the downstream events in chondrogenesis using *Hyp* mice, the murine homolog of human X-linked hypophosphatemia. *Hyp* mice showed reduced apoptosis and mineralization in hypertrophic cartilage. *Hyp* chondrocytes in culture displayed decreased apoptosis and mineralization compared with WT chondrocytes, whereas glycosaminoglycan synthesis, an early event in chondrogenesis, was not altered. Expression of the type III NPT *Pit-1* and P_i uptake were diminished, and intracellular ATP levels were also reduced in parallel with decreased caspase-9 and caspase-3 activity in *Hyp* chondrocytes. The competitive NPT inhibitor phosphonoformic acid and ATP synthesis inhibitor 3-bromopyruvate disturbed endochondral ossification with reduced apoptosis *in vivo* and suppressed apoptosis and mineralization in conjunction with reduced P_i uptake and ATP synthesis in WT chondrocytes. Overexpression of *Pit-1* in *Hyp* chondrocytes reversed P_i uptake and ATP synthesis and restored apoptosis and mineralization. Our results suggest that cellular ATP synthesis consequent to P_i uptake via *Pit-1* plays an important role in chondrocyte apoptosis and mineralization, and that chondrogenesis is ATP-dependent.

Endochondral ossification is critical to the development and growth of mammals. The process begins with condensation of undifferentiated mesenchymal cells, and these cells differentiate into proliferating chondrocytes that express type II, IX, and XI collagen and sulfated glycosaminoglycans (GAG)[2] (1). Proliferating chondrocytes further differentiate into hypertrophic chondrocytes expressing type X collagen, undergo apoptosis, mineralize, and are ultimately replaced by bone. Disturbance of the endochondral ossification leads to a variety of skeletal disorders.

The genetic disease X-linked hypophosphatemia (XLH) is the most common form of inherited rickets in humans and is related to the dominant disorder of P_i homeostasis (2). XLH has been shown to be caused by inactive mutations of the *PHEX* gene and characterized by hypophosphatemia secondary to renal P_i wasting, growth retardation due to disturbed endochondral ossification, osteomalacia resulting from reduced mineralization, and abnormally regulated vitamin D metabolism (3). *Hyp* mice also display similar biochemical and phenotypic abnormalities to human XLH, including hypophosphatemia, osteomalacia, and skeletal abnormalities. *Hyp* mice thus are a mouse homolog of human XLH (4). Previous studies reported that *Hyp* mice exhibited disorganized hypertrophic cartilage with reduced apoptotic chondrocytes and hypomineralization (5). We have reported previously that osteoclast number was decreased in *Hyp* mice compared with WT mice and that a high-P_i diet partially restored this, showing that P_i influences osteoclastogenesis and suggesting that this P_i effect on osteoclastogenesis may be associated with the pathogenesis of abnormal skeletogenesis in *Hyp* mice (6). However, it remains unclear whether disturbed P_i homeostasis influences endochondral ossification, leading to abnormal skeletogenesis in *Hyp* mice. In this context, it is noted that intracellular P_i levels decrease and extracellular P_i levels prominently increase from the proliferating to the hypertrophic zone during chondrogenesis, suggesting that cellular P_i levels are associated with chondrocyte differentiation (7–10).

Cellular P_i levels are controlled by the sodium-dependent P_i cotransporters (NPT) (11). Previous studies reported that the type III NPT *Pit-1* was expressed in hypertrophic chondrocytes during endochondral ossification in mice (12) and that the expression of the type IIa NPT *Npt2a* and *Pit-1* was also detected in chick chondrocytes (13). Moreover, it has been demonstrated that P_i modulates chondrocyte differentiation (14–19) and apoptosis (13, 20).

On the basis of these earlier results, we hypothesized that the NPT-P_i system plays a critical role in the regulation of chondrocyte differentiation. We found that *Pit-1* expression in chondrocytes was decreased in *Hyp* mice compared with WT mice and that *Pit-1* regulated apoptosis and mineralization in chondrocytes through modulating intracellular ATP

* This work was supported in part by the 21st Century COE Program entitled "Origination of Frontier BioDentistry" at Osaka University Graduate School of Dentistry, by the Ministry of Education, Culture, Sports, Science, and Technology, and by Grant-in-aid for Scientific Research A202290100 from the Japanese Society for the Promotion of Science (to T. Y.).

[1] To whom correspondence should be addressed: 1-8 Yamadaoka, Suita, Osaka 565-0871, Japan. Fax: 81-6-6879-2890; E-mail: tyoneda@dent.osaka-u.ac.jp.

[2] The abbreviations used are: GAG, glycosaminoglycan(s); XLH, X-linked hypophosphatemia; NPT, sodium-dependent P_i cotransporter(s); PFA, phosphonoformic acid; 3-BrPA, 3-bromopyruvate; STC, stanniocalcin.

Downloaded from www.jbc.org at OSAKA UNIVERSITY, on May 28, 2012

synthesis and apoptotic signaling activity. On the other hand, *Hyp* chondrocytes showed no changes in GAG synthesis, which is an early event in chondrogenesis. Our findings suggest that ATP synthesis mediated by P_i influx via *Pit-1* is critical in the regulation of late chondrogenesis, including apoptosis and mineralization, and that the differentiation of cartilage is an ATP-dependent event.

EXPERIMENTAL PROCEDURES

Animals—All mice used were of the C57BL/6J strain. Normal mice were purchased from Nihon-Dobutsu Inc. (Osaka, Japan). *Hyp* mice were initially obtained from The Jackson Laboratory (Bar Harbor, ME) and were produced by crossmating homozygous *Hyp* females (*Hyp*/*Hyp*) with hemizygous *Hyp* males (*Hyp*/Y). All animal experiments were performed according to the guidelines of the Institutional Animal Care and Use Committee of the Osaka University Graduate School of Dentistry.

Isolation and Culture of Mouse Growth Plate Chondrocytes—Growth plate chondrocytes were isolated from the ribs of 4-week-old normal and *Hyp* mice by sequential digestion with 0.2% trypsin (Invitrogen) for 30 min and 0.2% collagenase (Wako Pure Chemical Industries Ltd., Osaka, Japan) for 3 h as reported previously (21). Isolated cells were plated onto 100-mm tissue culture dishes at a density of 1×10^6 cells in α-minimal essential medium (Sigma) supplemented with 10% FCS (Valley Biomedical, Inc., Winchester, VA), 2 mmol/liter L-glutamine, and 0.1 mg/ml kanamycin. Two days later, to induce chondrogenesis and cartilage nodule formation, the cells were plated at 3×10^5 cells/well onto 24-well plates or at 5×10^4 cells/well on 96-well plates coated with type I collagen (Nitta Gelatin Inc., Osaka, Japan) and cultured in differentiation medium consisting of DMEM (Sigma) supplemented with 10% FCS, 50 μg/ml ascorbic acid, and 100 ng/ml recombinant human bone morphogenetic protein-2 (Astellas Pharma Inc., Tokyo, Japan) for 7 days. From day 5 to day 7, to promote matrix mineralization, 5 mM β-glycerophosphate was added to the differentiation medium.

RT-PCR and Real-time PCR—Total RNA from chondrocytes was prepared using an RNeasy kit (Qiagen, Inc., Valencia, CA) and reverse-transcribed with SuperScript II reverse transcriptase (Invitrogen). The primer sequences for mouse *Npt1*, mouse *Npt2a*, GAPDH, and β-actin are available on request. PCR assays were performed using *Taq* DNA polymerase (New England Biolabs, Ipswich, MA) and dNTP mixture (Promega Corp., Madison, WI). Real-time PCR assays were performed using a LightCycler system (Roche Diagnostics) according to the manufacturer's instructions. Each reaction was carried out with Qiagen QuantiTect SYBR Green PCR Master Mix. The expression levels of mRNA are indicated as the relative expression normalized by GAPDH. The primer sequences are available upon request. Each procedure was repeated at least four times to assess reproducibility.

Measurement of Sodium-dependent P_i Uptake—Assay for sodium-dependent P_i uptake by growth plate chondrocytes was performed essentially as described (22). Briefly, confluent cells cultured in 24-well Costar microtiter dishes were incubated in 2 ml of uptake solution (150 mmol/liter NaCl, 1.0 mmol/liter $CaCl_2$, 1.8 mmol/liter $MgSO_4$, and 10 mmol/liter HEPES (pH 7.4)) at 37 °C for 5 min. Transport was then initiated by replacing the uptake solution with fresh uptake solution (2 ml) supplemented with 0.1 mmol/liter KH_2PO_4 and containing 3 μCi/ml $KH_2{}^{32}PO_4$ (MP Biomedicals, Inc., Irvine, CA). Cells were then incubated for 5 min at 37 °C, and the reaction was stopped by the addition of ice-cold uptake solution supplemented with 150 mmol/liter choline chloride substitution for NaCl. The same solution was then used to wash the cells three times (2 ml/wash) and dissolved in 0.2 N NaOH, and the ^{32}P activity was counted on a scintillation counter. As a control, sodium-independent P_i transport was measured in the same way, except that NaCl was replaced by choline chloride in the uptake solution. Data are expressed as nanomoles of P_i/mg of cellular protein/5 min, and sodium-dependent P_i transport was calculated by subtracting sodium-independent P_i transport from total P_i transport.

Alcian Blue Staining—Cell layers in 24-well plates were fixed with 3.7% formaldehyde for 10 min and with 70% ethanol for 5 min at room temperature. After fixation, the cells were incubated with 5% acetic acid (pH 1.0, adjusted with HCl) for 5 min and stained with 1% Alcian blue dye (Wako Pure Chemical Industries Ltd.) in 5% acetic acid for 10 min. The Alcian blue staining was quantified using NIH Image 1.63 software.

Alizarin Red Staining—Cell layers in 24-well plates were fixed with 3.7% formaldehyde for 10 min and with 95% ethanol for 10 min at room temperature. After fixation, mineralized nodules were stained with 1% alizarin red S (Wako Pure Chemical Industries Ltd.) at pH 6.4 for 10 min at room temperature. The stained samples were washed three times with water and then air-dried. The alizarin red staining was quantified using NIH Image 1.63 software.

Treatment with NPT Inhibitor—*In vitro*, chondrocytes were treated with phosphonoformic acid (PFA or foscarnet, Sigma), which is a competitive inhibitor of NPT (23), at concentrations of 10^{-5} to 10^{-3} M in the differentiation medium from day 1 to day 7. *In vivo*, mice received PFA as described (24). PFA injection (intraperitoneal; 1000 mg/kg of body weight) was started at 21 days of age and injected daily for 10 days into C57BL/6J mice. Histological analysis was performed at 31 days of age. Control mice received vehicle PBS.

Knockdown of Npt2a and Pit-1 by siRNA—Chondrocytes were seeded at a density of 5×10^5 cells in 100-mm tissue culture dishes in α-minimal essential medium supplemented with 10% FCS and 2 mmol/liter L-glutamine. The sequences of Stealth RNAi duplex oligoribonucleotides for mouse *Npt2a* and mouse *Pit-1* are available upon request. *Npt2a*-targeted, *Pit-1*-targeted, or negative control (medium GC, Invitrogen) Stealth RNAi duplex oligoribonucleotides were each added to 1 ml of serum-free Opti-MEM I reduced serum medium (Invitrogen) at a final concentration of 24 nM. In a separate tube, 20 μl of Lipofectamine RNAiMAX (Invitrogen) were diluted in 1 ml of serum-free Opti-MEM I reduced serum medium. After adding the siRNA solution to the Lipofectamine solution, the final transfection mixture was incubated for 20 min at room temperature. This transfection mixture was applied to the cells. After 48 h, RNA extraction was performed for

Downloaded from www.jbc.org at OSAKA UNIVERSITY, on May 28, 2012

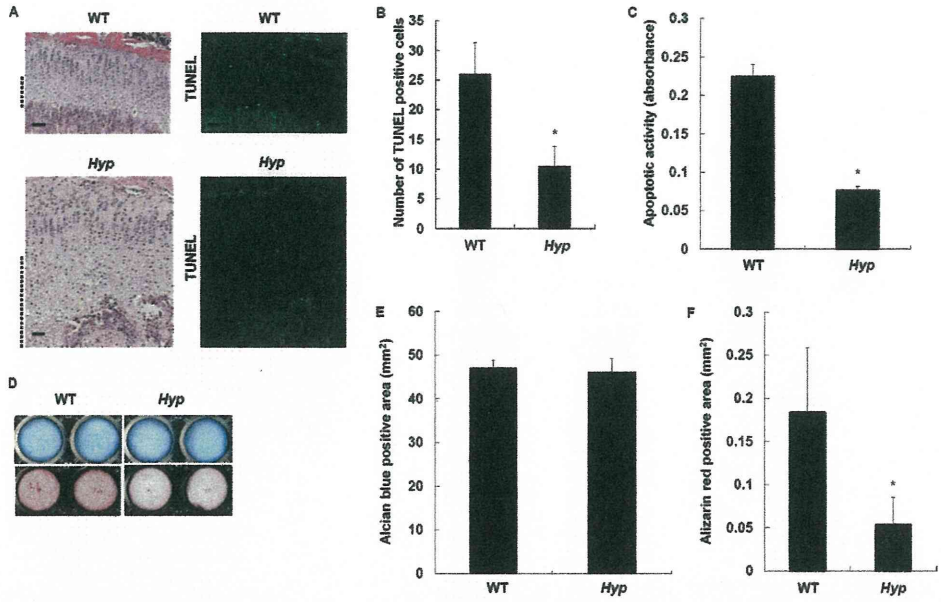

FIGURE 1. **Apoptosis and related events in *Hyp* chondrocytes.** *A*, histological examination of chondrocyte apoptosis. Hematoxylin/eosin staining (*left*) and TUNEL staining (*right*) were performed using tibias of 4-week-old WT and *Hyp* mice. The hypertrophic zone is marked with *dotted lines*, and the *scale bars* indicate 200 μm. Representative pictures obtained of numerous sections of four mice from each group are shown. *B*, number of TUNEL-positive cells in the tibial growth plates of WT and *Hyp* mice. *C*, quantitative determination of chondrocyte apoptosis. Cells were cultured in the differentiation medium in 96-well plates for 7 days. The determination was conducted using the cell death detection ELISA^{PLUS} kit after differentiation. Data are shown as apoptotic activity. *D*, histochemical staining of WT and *Hyp* chondrocytes. Cells were cultured for 7 days in the differentiation medium and stained with Alcian blue for GAG synthesis (*upper*) and with alizarin red S for mineralization (*lower*). *E*, quantification of Alcian blue staining. *F*, quantification of alizarin red staining. Results are expressed as the mean ± S.E. of four separate experiments. *, significantly different from WT chondrocytes ($p < 0.05$).

RT-PCR, and transfected chondrocytes were plated onto 24- or 96-well plates to determine P_i transport, intracellular ATP levels, caspase activity, and apoptosis.

Pit-1 Overexpression—The cDNA was subcloned into the 5′-XhoI/BamHI-3′ site of pcDNA3.1/Zeo (Invitrogen). The cells were transfected using FuGENE^{TM}-6 (Roche Diagnostics) according to the manufacturer's protocol. After 48 h of transfection, RNA extraction was performed for RT-PCR, or transfected chondrocytes were replated onto 24- or 96-well plates to determine P_i transport, intracellular ATP levels, caspase activity, and apoptosis. The cDNA for mouse *Pit-1* in the plasmid pBluescript was a generous gift of Dr. Kenichi Miyamoto (University of Tokushima Graduate School, Tokushima, Japan).

Histology and TUNEL Staining—Tibias were harvested, washed with PBS, fixed with 4% paraformaldehyde in 0.1 M phosphate buffer (pH 7.4) overnight, decalcified in 4.13% EDTA at room temperature for 2 weeks, and embedded in paraffin. Four-μm thick sections were made and stained with hematoxylin and eosin. Apoptotic cells were identified using the DeadEnd fluorometric TUNEL system (Promega Corp.). After treatment with 10 mg/ml proteinase K for 10 min at room temperature, sections were incubated with rTdT incubation buffer for 1 h at 37 °C, rinsed, counterstained with 1 μg/ml DAPI (Vector Laboratories, Ltd., Burlingame, CA), and mounted with Fluoromount-G (Southern Biotechnology Associates, Inc., Birmingham, AL). The green TUNEL emission was analyzed under a fluorescein filter set to view the green fluorescence of fluorescein at 520 nm and blue DAPI at 460 nm.

Measurement of Apoptotic Cell Death—DNA fragmentation was measured using the cell death detection ELISA^{PLUS} kit (Roche Diagnostics), which detects the cytoplasmic histone-associated DNA fragments (mono- and oligonucleosomes) by photometric enzyme immunoassay. Briefly, after differentiation of chondrocytes in 96-well plates, cell lysates were used for the ELISA procedure following the manufacturer's protocol. DNA fragmentation was quantified at 405 nm. Results were normalized to cellular protein concentration.

Measurement of Caspase-9 and Caspase-3 Activity—Activity of caspase-3 and caspase-9 was measured using the Caspase-Glo 3/7 and Caspase-Glo 9 assay kit (Promega corp.) according to the manufacturer's instructions. Chondrocytes were cultured at a density of 5×10^4 cells/well for 5 days in 96-well plates in the differentiation medium and processed for caspase-9 and caspase-3 activity assays. The luminescence was measured using a TD-20/20 luminometer (Tuner Designs, Sunnyvale, CA). Results were normalized to cellular protein concentration.

Measurement of Intracellular ATP Levels—Intracellular ATP levels were measured using an ATP assay kit (Calbiochem). This assay utilizes luciferase to catalyze the formation of light from ATP and luciferin. Luminescence was measured using a TD-20/20 luminometer. Chondrocytes were cultured at a density of 5×10^4 cells/well for 24 h in 24-well plates and processed for ATP bioluminescence assays. Results were normalized to cellular protein concentration.

Treatment with ATP Synthesis Inhibitor—*In vitro*, 3-bromopyruvate (3-BrPA; Sigma), a strong alkylating agent that abolishes cell ATP production via the inhibition of both gly-

Downloaded from www.jbc.org at OSAKA UNIVERSITY, on May 28, 2012

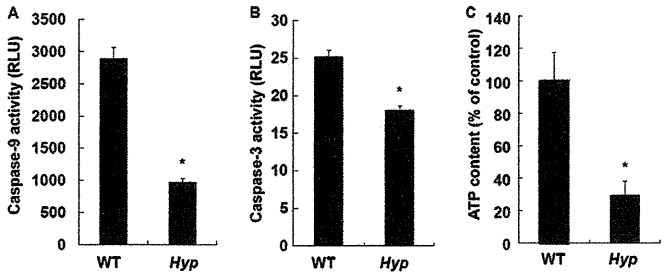

FIGURE 2. **Activity of apoptotic signaling pathways.** *A*, caspase-9 activity in WT and *Hyp* chondrocytes. *B*, caspase-3 activity in WT and *Hyp* chondrocytes. Activity was measured using the Caspase-Glo 9 and Caspase-Glo 3/7 assay kits after differentiation. *C*, intracellular ATP levels in WT and *Hyp* chondrocytes. Cells were cultured at a density of 1×10^4 cells/well in 96-well plates for 24 h. ATP levels were measured using the ATP assay kit. *, significantly different from WT chondrocytes ($p < 0.05$). *RLU*, relative light units.

colysis and oxidative phosphorylation (25–27), was added at 10^{-6}~10^{-5} M in the differentiation medium from day 1 to day 7. *In vivo*, 3-BrPA (20 μg/kg of body weight) was injected intraperitoneally daily for 10 days into C57BL/6J mice. Control mice received vehicle PBS.

Statistical Analysis—Data are presented as the mean ± S.E. Raw data were analyzed by the Mann-Whitney *U* test or one-way analysis of variance, followed by a post hoc test (Fisher's projected least significant difference) (StatView, SAS Institute, Inc., Cary, NC) with a significance level of $p < 0.05$.

RESULTS

Reduced Apoptosis and Mineralization in Growth Plate Cartilage in Hyp Mice—It has been reported that apoptosis is a prerequisite to mineralization of chondrocytes (28). Previous studies, including ours, have reported that the growth plate cartilage in *Hyp* mice is hypomineralized (5, 6). We therefore examined apoptosis in the growth plate cartilage in *Hyp* mice compared with WT mice. Histological examination revealed that hypertrophic cartilage was elongated and disorganized in *Hyp* mice (Fig. 1*A*, *left*). In conjunction with this, TUNEL staining showed decreased apoptosis in hypertrophic cartilage in *Hyp* mice (Fig. 1, *A* (*right*) and *B*). Consistent with these *in vivo* results, chondrocytes isolated from *Hyp* mice (*Hyp* chondrocytes) in culture showed decreased apoptosis assessed by DNA fragmentation using a commercially available ELISA kit (Fig. 1*C*), and mineralization was determined by alizarin red staining (Fig. 1*D*, *lower*). Quantification of alizarin red staining is shown in Fig. 1*F*. However, GAG synthesis, which takes place at an early stage of chondrogenesis, was not altered in *Hyp* chondrocytes as determined by Alcian blue staining (Fig. 1*D*, *upper*) Alcian blue staining is quantified in Fig. 1*E*.

Cellular Events Involved in Reduced Apoptosis in Hyp Chondrocytes—Because activation of caspase-9 and caspase-3 is an important step that leads to apoptosis, the activity of caspase-9 and caspase-3 was next determined in WT and *Hyp* chondrocytes in culture. The activity of caspase-9 (Fig. 2*A*) and caspase-3 (Fig. 2*B*) was significantly decreased in *Hyp* chondrocytes. ATP has been reported to be critical in the activation of caspase-9 and caspase-3 (29, 30). Accordingly, we determined intracellular ATP levels in WT and *Hyp* chondrocytes and found that intracellular ATP levels in *Hyp* chondrocytes were significantly reduced compared with WT chondrocytes (Fig. 2*C*). Collectively, these results suggest that decreased ATP levels impaired caspase signals following apoptosis in *Hyp* chondrocytes.

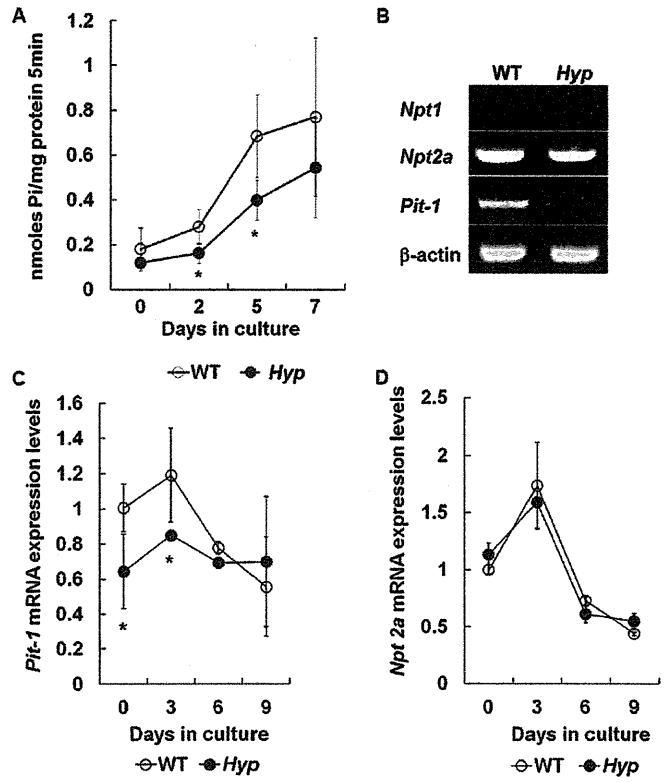

FIGURE 3. **Characterization of *Hyp* chondrocytes.** *A*, time course of P_i uptake in WT (○) and *Hyp* (●) chondrocytes. The cells were cultured for 7 days in the differentiation medium, and P_i uptake was determined as described under "Experimental Procedures." *B*, expression of *Npt1*, *Npt2a*, and *Pit-1* mRNAs in WT and *Hyp* chondrocytes. Total RNA isolated from chondrocytes cultured for 24 h was used for RT-PCR analysis using the primer pairs. β-Actin was amplified as a control. *C*, time-dependent expression of *Pit-1* mRNA by real-time PCR. *D*, time-dependent expression of *Npt2a* mRNA by real-time PCR. The amount of *Npt2a* and *Pit-1* of WT chondrocytes at day 0 was designated as 1.0 and normalized to GAPDH. Results are expressed as the mean ± S.E. of four separate experiments. *, significantly different from WT chondrocytes ($p < 0.05$).

Disturbed P_i Homeostasis in Hyp Chondrocytes—It has been described that P_i is a source of ATP (31). Accordingly, we next examined whether P_i uptake was changed in *Hyp* chondrocytes. As expected, we found that P_i uptake was significantly less in *Hyp* chondrocytes than in WT chondrocytes (Fig. 3*A*). Because cellular P_i uptake is under the control of NPT (11), NPT expression in *Hyp* chondrocytes was subsequently determined. RT-PCR showed that the type III NPT *Pit-1* expression was decreased in *Hyp* chondrocytes (Fig. 3*B*), and real-time PCR demonstrated that *Pit-1* expression was reduced at the early stages of chondrocyte culture (Fig. 3*C*). Consistent with our results, previous studies also reported that an increase in *Pit-1* expression at an early stage was associated with late chondrocyte differentiation (16, 18). On the other hand, there was no difference in the type II *Npt2a* expression between WT and *Hyp* chondrocytes (Fig. 3, *B* and *D*). The type I *Npt1* expression was not detected in WT and *Hyp* chondrocytes (Fig. 3*B*). These results suggest that P_i up-

Downloaded from www.jbc.org at OSAKA UNIVERSITY, on May 28, 2012